

RESEARCH ARTICLE

IL-27 signalling regulates glycolysis in Th1 cells to limit immunopathology during infection

Marcela Montes de Oca^{1‡}, Fabian de Labastida Rivera¹, Clay Winterford², Teija C. M. Frame¹, Susanna S. Ng¹, Fiona H. Amante¹, Chelsea L. Edwards¹, Luzia Bukali¹, Yulin Wang¹, Jude E. Uzonna³, Rachel D. Kuns⁴, Ping Zhang⁴, Agnieszka Kabat⁵, Ramon I. Klein Geltink⁵, Edward J. Pearce⁵, Geoffrey R. Hill⁶, Christian R. Engwerda^{1*}

1 Immunology and Infection Laboratory, Infectious Diseases Division, QIMR Berghofer Medical Research Institute, Brisbane, Australia, **2** QIMR Berghofer Histology Facility, QIMR Berghofer Medical Research Institute, Brisbane, Australia, **3** Department of Immunology, College of Medicine, University of Manitoba, Winnipeg, Manitoba, Canada, **4** Bone Marrow Transplantation Laboratory, Cancer Division, QIMR Berghofer Medical Research Institute, Brisbane, Australia, **5** Max Plank Institute of Immunobiology and Epigenetics, Freiburg, Germany, **6** Clinical Research Division, Fred Hutchinson Cancer Research Centre, Washington, United States of America

‡ Current address: York Biomedical Research Institute, Hull York Medical School, University of York, United Kingdom

* christian.engwerda@qimrberghofer.edu.au



OPEN ACCESS

Citation: Montes de Oca M, de Labastida Rivera F, Winterford C, Frame TCM, Ng SS, Amante FH, et al. (2020) IL-27 signalling regulates glycolysis in Th1 cells to limit immunopathology during infection. *PLoS Pathog* 16(10): e1008994. <https://doi.org/10.1371/journal.ppat.1008994>

Editor: Phillip Scott, University of Pennsylvania, UNITED STATES

Received: June 9, 2020

Accepted: September 18, 2020

Published: October 13, 2020

Copyright: © 2020 Montes de Oca et al. This is an open access article distributed under the terms of the [Creative Commons Attribution License](https://creativecommons.org/licenses/by/4.0/), which permits unrestricted use, distribution, and reproduction in any medium, provided the original author and source are credited.

Data Availability Statement: All relevant data are within the manuscript and its Supporting Information files.

Funding: This work was made possible through the QIMR Berghofer SEED funding grant (MM), Queensland State Government funding and grants and fellowships from the National Health and Medical Research Council of Australia (NHMRC; grant numbers 1132975 and 1154265) (CRE). The funders had no role in study design, data collection

Abstract

Inflammation is critical for controlling pathogens, but also responsible for symptoms of infectious diseases. IL-27 is an important regulator of inflammation and can limit development of IFN γ -producing Tbet⁺ CD4⁺ T (Th1) cells. IL-27 is thought to do this by stimulating IL-10 production by CD4⁺ T cells, but the underlying mechanisms of these immunoregulatory pathways are not clear. Here we studied the role of IL-27 signalling in experimental visceral leishmaniasis (VL) caused by infection of C57BL/6 mice with the human pathogen *Leishmania donovani*. We found IL-27 signalling was critical for the development of IL-10-producing Th1 (Tr1) cells during infection. Furthermore, in the absence of IL-27 signalling, there was improved control of parasite growth, but accelerated splenic pathology characterised by the loss of marginal zone macrophages. Critically, we discovered that IL-27 signalling limited glycolysis in Th1 cells during infection that in turn attenuated inflammation. Furthermore, the modulation of glycolysis in the absence of IL-27 signalling restricted tissue pathology without compromising anti-parasitic immunity. Together, these findings identify a novel mechanism by which IL-27 mediates immune regulation during disease by regulating cellular metabolism.

Author summary

Infectious diseases like visceral leishmaniasis caused by the protozoan parasites *Leishmania donovani* and *L. infantum* are associated with an inflammatory response generated by the host. This is needed to control parasite growth, but also contributes to the symptoms of disease. Consequently, these inflammatory responses need to be tightly regulated.

and analysis, decision to publish, or preparation of the manuscript.

Competing interests: The authors have declared that no competing interests exist.

Although we now recognize many of the cells and molecules involved in controlling inflammation, the underlying mechanisms mediating immune regulation are unclear. CD4⁺ T cells are critical drivers of inflammatory responses during infections and as they progress from a naïve to activated state, the metabolic pathways they use have to change to meet the new energy demands required to proliferate and produce effector molecules. In this study, we discovered that the inflammatory CD4⁺ T cells needed to control *L. donovani* infection switch from relying on mitochondrial oxidative pathways to glycolysis. Critically, we found the cytokine IL-27 limited glycolysis in these inflammatory CD4⁺ T cells, and in the absence of IL-27 signaling pathways, these cells expanded more rapidly to better control parasite growth, but also caused increased tissue damage in the spleen. However, pharmacological dampening of glycolysis in inflammatory CD4⁺ T cells in *L. donovani*-infected mice lacking IL-27 signaling pathways limited tissue damage without affecting their improved anti-parasitic activity. Together, these results demonstrate that the pathogenic activity of inflammatory CD4⁺ T cells can be modulated by altering their cellular metabolism.

Introduction

Inflammation is a critical physiological process that mediates protection against invading pathogens. Immunoregulatory mechanisms limit inflammatory responses to prevent host tissue damage. Visceral leishmaniasis (VL) caused by *Leishmania donovani* and *L. infantum* is characterised by the development of a potent inflammatory response [1–3], which limits parasite growth but can also damage tissue (reviewed in [4]). A clinical feature of VL patients is hepatosplenomegaly [3, 4], which is associated with disease complications such as secondary infections, anaemia, and malnutrition, all of which can contribute to VL mortality [3–5].

Experimental VL caused by *L. donovani* infection in genetically susceptible mice is a useful model to study inflammation in the context of acute and chronic infection within the same host because the liver is a site of acute infection whereas chronic infection becomes established in the spleen [6,7]. Infection in the liver stimulates an inflammatory cascade including the early recruitment of innate immune cells, followed by T cells, and the rapid proliferation of the recruited lymphocytes [8]. Liver inflammation also promotes oedema, increasing the distance between parenchymal cells and blood vessels, resulting in a nutrient- and oxygen-poor micro-environment [8]. Therefore, T cells travelling from nutrient-rich secondary lymphoid tissues, such as the spleen and lymph nodes, to these sites of inflammation must adapt their metabolism to maintain their effector functions at low oxygen and nutrient levels [9]. Furthermore, the development of splenomegaly in both human and experimental VL is associated with cellular expansion and tissue reorganisation, and is likely to have consequences for cellular metabolism that are currently unclear [10,11].

We previously reported a role for Blimp-1 in inducing IL-10 production by Th1 cells to become type 1 regulatory T (Tr1) cells that protected against IFN γ - and TNF-mediated splenic pathology during infection [12]. We have also shown that CD4⁺ T cells were a major source of IL-10 that protected against tissue damage during *L. donovani* infection [12,13]. A link between IL-27 signalling, Tr1 cell development and IL-10 mediated control of immunopathology has been extensively reported [14–24]. However, in some instances, IL-27 can also promote inflammation by preventing regulatory T (Treg) cell expansion [25]. Hence, a better understanding about the induction and maintenance of IL-27-mediated immunoregulatory pathways is needed if they are to be exploited clinically.

IL-27p28 and Ebi3 combine to form the IL-27 heterodimer [26] that signals via the IL-27 receptor (IL-27R) composed of IL-27R α and gp130 [27]. The engagement of IL-27 to its receptor causes phosphorylation of JAK1/2 or TYK2 and signalling via STAT1 and STAT4 to stimulate *TBET* and *IFNG* gene transcription, respectively [28,29]. Alternatively, signalling via STAT3 can induce *IL10* gene transcription [16,24,30]. A previous study reported that *Il27ra*^{-/-} mice developed liver damage mediated by CD4⁺ T cells and excessive IFN γ and TNF production following *L. donovani* infection, indicating an important role for IL-27 in protecting tissue from excess inflammation [5]. *Il27p28* and *Ebi3* mRNA levels were also reported to be significantly elevated in VL patient plasma, compared to endemic controls and CD14⁺ cells were identified as the main source of IL-27 [15].

In addition to protecting against tissue damage, IL-27 was postulated to promote susceptibility to VL by suppressing IL-17-mediated neutrophil recruitment. *Ebi3*^{-/-} mice had reduced IFN γ levels, compared to wild type controls, but lower parasite burdens associated with exacerbated IL-17A production leading to a greater neutrophil influx [31]. In humans, the severity of VL caused by *L. infantum* positively correlated with serum IL-6, IL-27 and sCD14 levels [32]. Similarly, there was a strong association between serum IFN γ , IL-27, IL-10, IL-6 and sCD14 levels and the degree of hepatosplenomegaly, neutropenia and thrombocytopenia in VL patients infected with *L. infantum* [32]. However, despite these reports, the cellular and molecular mechanisms underpinning IL-27 functions during VL remains poorly understood.

Cellular metabolism is tightly linked with immune cell function. Nutrient and oxygen availability, activation status, tissue site and transcriptional programming combine to orchestrate a functional immune response. Naïve CD4⁺ T cells favour energy production over biosynthesis and generally rely on mitochondrial oxidative pathways, fuelled by fatty acid or amino acid oxidation [33]. Differentiated Th1 cells rely on glycolysis and glutaminolysis to support their growth and proliferation, where α -ketoglutarate has been postulated to act as a metabolic regulator by promoting *Tbet* expression and mTORC1 signalling [34,35]. Glucose uptake and aerobic glycolysis is essential for IFN γ production by Th1 cells [36,37]. Metabolic reprogramming to glycolysis accommodates for an increase in biomass to cope with the new energy demands of the cell, but also allows for the generation of metabolic intermediates that feed into other biosynthetic pathways, such as the pentose phosphate pathway or TCA cycle. However, the mechanisms controlling these changes in CD4⁺ T cell metabolism remain poorly defined.

Here, we examined the role of IL-27 signalling in regulating CD4⁺ T cell differentiation and balancing anti-parasitic immunity and tissue pathology in experimental VL caused by *L. donovani* infection of C57BL/6 mice. We identified IL-27 as an important regulator of glycolysis in Th1 cells that limited host tissue damage in the spleen following infection. Importantly, we demonstrate that modulation of glycolysis during infection has therapeutic potential to reduce tissue damage without compromising control of parasite growth.

Results

IL-27 signalling impedes control of parasite growth and determines the balance between Th1 and Tr1 cells during infection

To better understand the role of IL-27 signalling in the development of anti-parasitic immunity during VL, we infected *Il27ra*-deficient C57BL/6 (*Il27ra*^{-/-}) and wild-type (WT) C57BL/6 control mice with *L. donovani* and examined disease outcomes. Consistent with previous findings [5], *Il27ra*^{-/-} mice had significantly increased spleen and liver weights 14 days post infection (p.i.), compared to WT controls, indicating early development of tissue pathology (Fig 1A and 1B). However, we also noted reduced parasite burdens in the spleen and liver, associated with increased numbers of antigen specific CD4⁺ T cells and Th1 cells, relative to WT controls

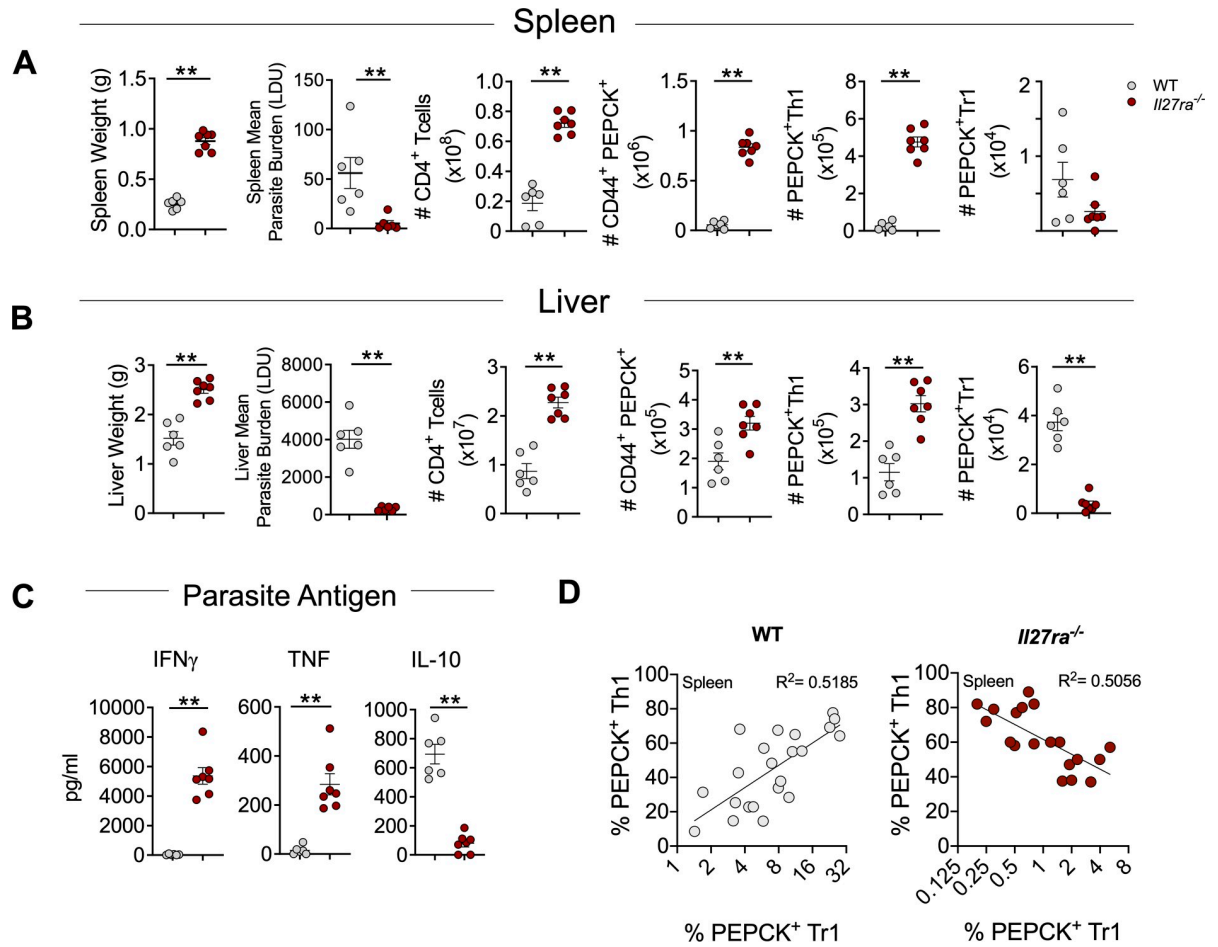


Fig 1. IL-27 signalling impedes control of parasite growth and determines the balance between Th1 and Tr1 cells during infection. WT and *Il27ra*^{-/-} mice were infected with 2x10⁷ *L. donovani* amastigotes i.v.. Organ pathology, parasite burdens and cellular immune responses were measured in both the spleen (A) and liver 14 days p.i. (B). (A) Left to right: spleen weights shown in grams (g). Parasite burdens in the spleen were expressed by Leishman Donovan Units (LDU) where organ weight is multiplied by the number of parasites per 1000 nuclei in each organ. CD4⁺ T cell numbers were measured by flow cytometry as CD4⁺ TCR β ⁺. Antigen specific CD4⁺ T cell numbers defined as CD44⁺ PEPCK⁺. Antigen specific Th1 cell numbers defined as CD44⁺ PEPCK⁺ Tbet⁺ IFN γ ⁺. Antigen specific Tr1 cell numbers defined as CD44⁺ PEPCK⁺ IL-10⁺ IFN γ ⁺. (B) Left to right: liver weights shown in grams (g). Parasite burdens in the liver were expressed by Leishman Donovan Units (LDU). CD4⁺ T cell numbers are shown. Antigen specific CD4⁺ T cell numbers are shown. Antigen specific Th1 cell numbers are shown. Antigen specific Tr1 cell numbers are shown. (C) Splenocytes were cultured with or without the presence of *L. donovani* antigen and cytokines in culture supernatants were measured by CBA, 72 hours post re-stimulation. (D) WT (n = 22) and *Il27ra*^{-/-} (n = 19); Correlation of antigen-specific Th1 cells and antigen-specific Tr1 cells in the spleens of WT and *Il27ra*^{-/-} mice at day 14 p.i. shown by linear regression analysis. Data shown is representative of 3 independent experiments performed with n = 6–7 mice per group, in each experiment and are presented as mean \pm SEM, **p<0.01, Mann-Whitney U test.

<https://doi.org/10.1371/journal.ppat.1008994.g001>

(Fig 1A and 1B, S1A–S1C Fig), as well as elevated levels of IFN γ and TNF in the serum of infected *Il27ra*^{-/-} mice, compared to WT controls (S1D Fig). Antigen-specific CD4⁺ T cells were measured using the PEPCK₃₃₅₋₃₅₁ tetramer comprising a parasite peptide found in all pathogenic *Leishmania* species [38] (S1A and S1B Fig). Interestingly, we found reduced numbers of PEPCK⁺ Tr1 cells in the liver (Fig 1B), and reduced frequencies of Tr1 cells in both spleen and liver *Il27ra*^{-/-} mice, compared to WT mice (S1C Fig). This was accompanied by an increased frequency of polyclonal Th1 cells in *L. donovani*-infected *Il27ra*^{-/-} mice compared to infected WT mice (S1F Fig). In addition, IFN γ and TNF levels were elevated, and IL-10 levels were reduced following stimulation of splenocytes from *Il27ra*^{-/-} mice relative to WT mice

with parasite antigen at day 14 p.i. (Fig 1C). Therefore, we hypothesised that the more rapid development of splenomegaly in *L. donovani*-infected *Il27ra*^{-/-} mice was caused by an unbalanced Th1 and Tr1 cell response. This was supported by an inverse correlation between antigen-specific Th1 and Tr1 cell frequency in *Il27ra*^{-/-} mice in the spleen 14 days p.i., as opposed to the positive correlation apparent in WT controls (Fig 1D).

To establish whether IL-27 signalled directly to macrophages to affect their ability to control parasite growth, we isolated peritoneal macrophages from *Il27ra*^{-/-} mice and WT controls, infected them and then cultured them with or without IFN γ . We found no impact of *Il27ra*-deficiency on the establishment of infection or growth of parasites in host macrophages (S1G Fig). Furthermore, the addition of IFN γ resulted in improved control of parasite growth in both *Il27ra*^{-/-} and WT macrophages, while the addition of IL-27 had no significant impact on the establishment of infection or growth of parasites in WT macrophages (S1G Fig). Together, these data indicate that the increased hepatosplenomegaly associated with *L. donovani* infection in *Il27ra*^{-/-} mice relative to WT controls was not related to direct IL-27 signalling to infected macrophages, but instead was strongly associated with changes in the balance between Th1 and Tr1 cells.

IL-27 signalling protects splenic tissue against IFN γ - and TNF-mediated pathology during infection

L. donovani infected *Il27ra*^{-/-} mice have previously been shown to develop CD4⁺ T cell-mediated liver pathology [5]. During VL, splenomegaly is characterised by white pulp hyperplasia and IFN γ - and TNF-mediated killing of marginal zone macrophages, resulting in dysregulated lymphocyte trafficking [39]. Similar to our previous findings in *L. donovani*-infected mice with impaired development of Tr1 cells [12], *Il27ra*^{-/-} mice exhibited a significant loss of marginal zone macrophages (MZM) 14 days p.i., compared to infected WT mice (Fig 2A and 2B). The decrease in MZM numbers was not simply a result of tissue or cellular expansion caused by splenomegaly in *Il27ra*^{-/-} mice because when MZM numbers were normalised to spleen weight or cell number, the same pattern of MZM loss was observed (Fig 2B). As mentioned above, a likely explanation for the increased splenic pathology observed in *Il27ra*^{-/-} mice was the increased ratio of Th1:Tr1 cells in these mice following *L. donovani* infection, compared to WT animals (Fig 1D), although cytokine blocking studies in *Il27ra*^{-/-} mice are needed to confirm this.

IL-27 signalling mediates mitochondrial changes in the spleen but not liver during infection

Cellular metabolism is critical in shaping immune responses during infection. Naïve T cells predominantly use oxidative phosphorylation and once activated upregulate glycolysis to cope with the energy demands of newly activated cells [40]. During *L. donovani* infection, chronic infection becomes established in the spleen, whereas the liver is a site of self-resolving infection mediated by a Th1 cell-dominated granulomatous response [41–43]. To explore whether IL-27 signalling was associated with changes in CD4⁺ T cell metabolism during infection, we first measured mitochondrial mass and membrane potential using MitoTracker dyes in WT and *Il27ra*^{-/-} CD4⁺ T cells and Th1 cells 14 days after *L. donovani* infection. Here, we defined Th1 cells as CD4⁺ TCR β ⁺ CXCR3⁺ CXCR5⁻ as surrogate surface markers due to the sensitivity of MitoTracker dyes to fixation and permeabilization methods (S1E Fig). We found that *Il27ra*^{-/-} CD4⁺ T cells and Th1 cells had a two-fold increase in the MitoTracker Green⁺ MitoTracker Deep Red^{lo} population in the spleen (Fig 3A and 3B), but not the liver (Fig 3E and 3F), compared to the same cell populations from WT mice. Interestingly, this MTG⁺ MTD^{lo}

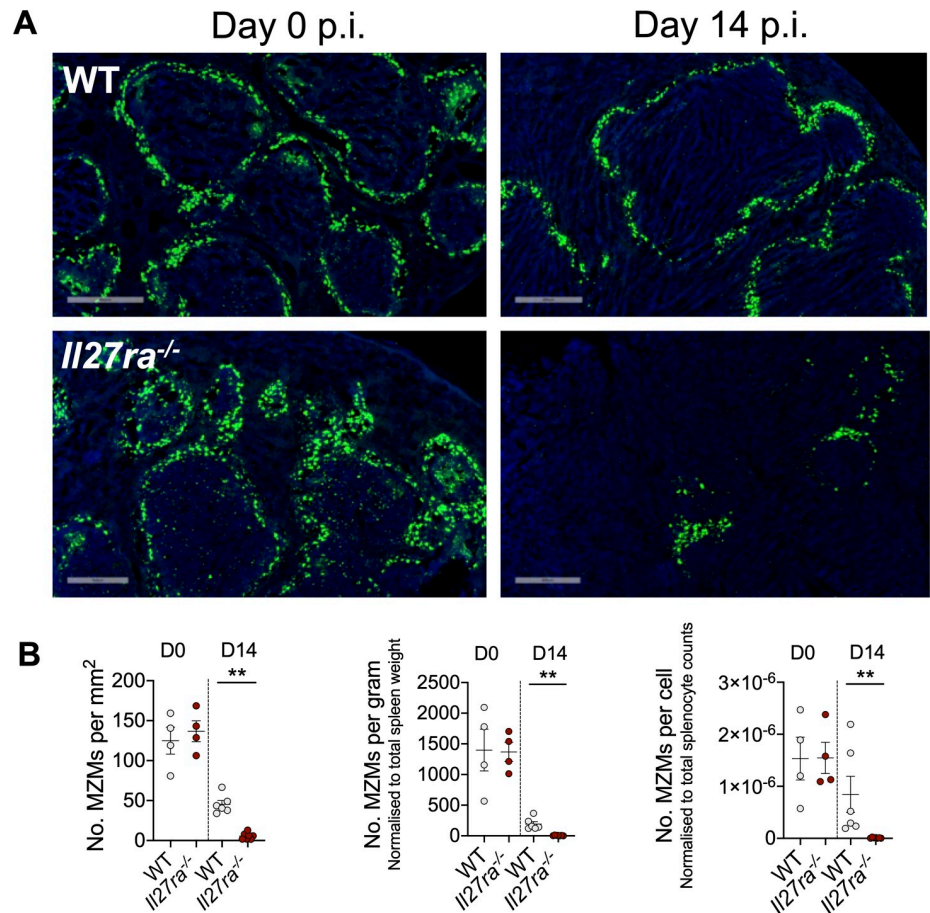


Fig 2. IL-27 signalling protects splenic architecture against TNF-mediated pathology during infection. (A) WT and *Il27ra*^{-/-} mice were infected with 2×10^7 *L. donovani* amastigotes i.v.. Mice were injected with 100 μ g of FITC dextran (in saline) i.v. and euthanized 2 hours later. Spleens harvested on day 0 and day 14 p.i.. (B) Marginal zone macrophages (MZMs) were quantified in 20 μ m thick sections using Metamorph software as total number of marginal zone macrophages (MZMs) per millimetre squared, normalised to total spleen weight and to total splenocyte counts. Scale bar: 500 μ m. Data shown is representative of 2 independent experiments performed with $n = 4-7$ mice per group, in each experiment and are presented as mean \pm SEM, ** $p < 0.01$, Mann-Whitney U test.

<https://doi.org/10.1371/journal.ppat.1008994.g002>

population in the spleen of *Il27ra*-deficient mice exhibited a dramatic increase in mROS expression measured by MitoSOX Red (Fig 3A–3C), indicative of highly activated CD4⁺ T cells [44,45]. Therefore, we hypothesised that the increased ROS production in *Il27ra*^{-/-} CD4⁺ T cells, and in particular Th1 cells, was due to the increased activation status of these cells, relative to WT cells. In support of this idea, we found CD4⁺ T cells from the spleens of *Il27ra*^{-/-} mice were larger in size and granularity, compared to the same cells from WT controls (Fig 3D), and again these differences were not found in the liver (Fig 3G and 3H). Collectively, these data indicate that IL-27 signalling suppressed mitochondrial changes in splenic CD4⁺ T cells during *L. donovani* infection that limit their activation status, potentially contributing to the immunosuppression observed in this tissue [46]. Furthermore, these mitochondrial changes observed in splenic CD4⁺ T cells were not simply caused by an increase in Th1 cell frequencies in *Il27ra*^{-/-} mice because we also observed these changes in MTG⁺ MTDR⁺ Th1 cells between WT and *Il27ra*^{-/-} mice. The minimal differences observed between WT and *Il27ra*^{-/-} CD4⁺ T cells and Th1 cells in the liver reflects the improved control of parasite load in this tissue, compared to the spleen [11, 43, 46]. We hypothesised that at day 14 p.i. when parasite load

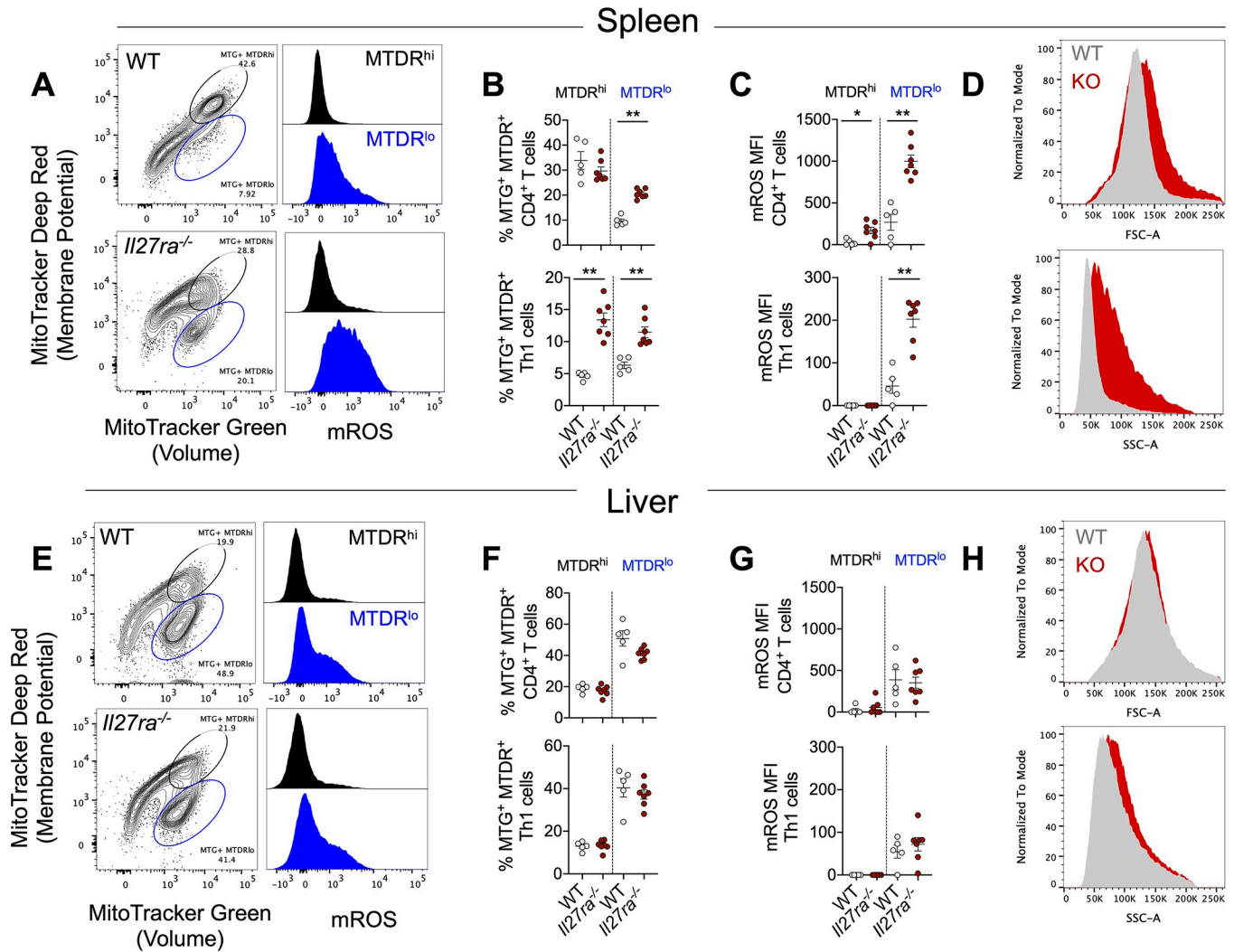


Fig 3. IL-27 signalling mediates mitochondrial changes in the spleen but not the liver during infection. (A, E) WT and *Il27ra*^{-/-} mice were infected with 2x10⁷ *L. donovani* amastigotes i.v.. Spleen and liver cells were harvested and stained for CD4, TCRβ, CXCR3 and CXCR5 along with MitoTracker Green (volume), MitoTracker DeepRed (membrane potential) and MitoSOX (mitochondrial ROS) to assess mitochondria in CD4⁺ T cells by flow cytometry. All plots are gated on CD4⁺ T cells. MTDR^{hi} (black gate and histogram), MTDR^{lo} (blue gate and histogram). CD4⁺ T cells defined as CD4⁺ TCRβ⁺ and Th1 cells defined as CD4⁺ TCRβ⁺ CXCR3⁺ CXCR5⁺ (B, F) Mitochondrial mass and membrane potential are shown as MitoTracker Green⁺ MitoTracker DeepRed⁺ on CD4⁺ T cells and Th1 cells at day 14 p.i.. (C, G) Mitochondrial Reactive Oxygen Species (mROS) measured by flow cytometry on CD4⁺ T cells and Th1 cells at day 14 p.i.. (D, H) Forward (FSC-A) and size scatter (SSC-A) histogram plots, WT (grey) and *Il27ra*^{-/-} (red). Data shown is representative of 2 independent experiments performed with n = 5–7 mice per group, in each experiment and are presented as mean ± SEM, **p<0.01, *p<0.05, Mann-Whitney U test.

<https://doi.org/10.1371/journal.ppat.1008994.g003>

begins to resolve in the liver, but not the spleen, the activation and metabolic potential of hepatic CD4⁺ T cells had already reached their maximum, hence no further increase in mROS or cell size and granularity was observed.

Th1 cells are more glycolytic than Tr1 cells in vivo

We next investigated how IL-27 signalling affects mitochondrial respiration in response to glucose. In CD4⁺ T cells from the spleen, we measured improved mitochondrial respiration (oxygen consumption rate, OCR) in response to glucose, in the absence of IL-27 signalling (S2A Fig), whereas minimal differences in OCR between WT and *Il27ra*^{-/-} CD4⁺ T cells were found in the liver (S2B Fig), supporting the above findings of tissue-specific differences in the

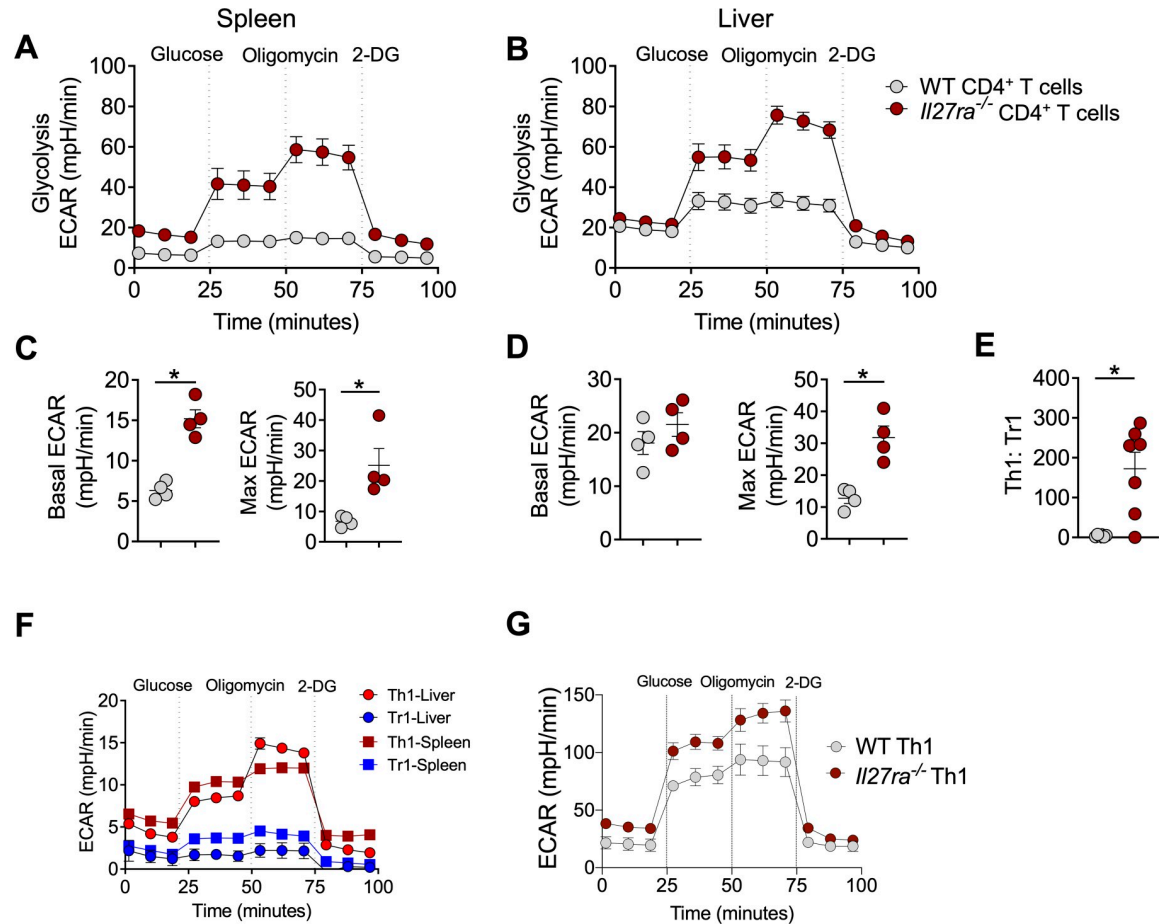


Fig 4. Th1 cells are more glycolytic than Tr1 cells in vivo during infection. WT and *Il27ra*^{-/-} mice were infected with 2×10^7 *L. donovani* amastigotes i.v.. Splenic and hepatic CD4⁺ T cells were MACS purified and assayed on the Seahorse XF96 using the glycolysis stress test kit at day 14 p.i. *ex vivo*. Total extracellular acidification rate (ECAR) was assessed after the addition of glucose, oligomycin and 2-DG at indicated times in the (A) spleen and (B) liver. Basal ECAR and maximal glycolysis (final measurement after the last oligomycin injection–final measurement after the last glucose injection) measured in the (C) spleen and (D) liver. (E) Th1:Tr1 cell ratio determined by flow cytometry. (F) *Il10gfp x Ifngyfp x foxp3rfp* mice were infected with 2×10^7 *L. donovani* amastigotes i.v.. Splenic and hepatic CD4⁺ T cells were sorted on the ARIA III for Th1 (IFN γ ⁺ IL-10⁻) and Tr1 (IFN γ ⁺ IL-10⁺) cells 14 days p.i.. Total extracellular acidification rate (ECAR) was assessed after the addition of glucose, oligomycin and 2-DG at indicated times in the spleen and liver *ex vivo*. (G) Splenic CD4⁺ T cells MACS purified from uninfected WT and *Il27ra*^{-/-} mice and polarised under Th1 conditions for 72 hours and then assayed on the Seahorse XF96. Glycolysis (ECAR) measured in all conditions. Data shown is representative of 2 independent experiments performed with $n = 3-7$ mice per group, in each experiment and are presented as mean \pm SEM, * $p < 0.05$, Mann-Whitney U test.

<https://doi.org/10.1371/journal.ppat.1008994.g004>

metabolic status of CD4⁺ T cells, where it appears that hepatic CD4⁺ T cells reached their peak metabolic state earlier than splenic CD4⁺ T cells. However, we found increased aerobic glycolysis (extracellular acidification rate, ECAR) in the absence of IL-27 signalling in CD4⁺ T cells from both spleen (Fig 4A) and liver (Fig 4B). Interestingly, *Il27ra*^{-/-} CD4⁺ T cells from the spleen were significantly more glycolytic than their WT counterparts, even at baseline (Fig 4C). Basal ECAR (absence of glucose) between WT and *Il27ra*^{-/-} CD4⁺ T cells in the liver was not different, and only when glucose became available in saturated amounts, did we observe a difference in glycolysis between WT and *Il27ra*^{-/-} CD4⁺ T cells (Fig 4D). Thus, despite differences in glucose utilisation between WT and *Il27ra*^{-/-} CD4⁺ T cells in the liver and spleen at baseline, the addition of a saturating amount of glucose resulted in the rapid breakdown of

glucose into pyruvate, measured by the maximum ECAR (Fig 4C and 4D). The number of live WT and *Il27ra*^{-/-} CD4⁺ T cells recovered and assayed was similar (~80%), and therefore did not account for the above differences at baseline. However, we cannot say whether these cells were more or less susceptible to cell death during the assay itself. Furthermore, once this glycolytic pathway was activated, *Il27ra*^{-/-} CD4⁺ T cells were significantly more glycolytic compared to WT cells in both tissues, as indicated by the max ECAR readings (Fig 4C and 4D). Because we measured aerobic glycolysis on bulk CD4⁺ T cell populations from WT and *Il27ra*^{-/-} mice, it is important to note that *Il27ra*^{-/-} mice exhibit a significantly higher Th1:Tr1 ratio (Fig 4E). Hence, differences in the capacity for aerobic glycolysis between Th1 and Tr1 cells may help to explain the increased ECAR in *Il27ra*^{-/-} CD4⁺ T cells, particularly in the liver (Fig 4B). Indeed, we found Th1 cells were more glycolytic than Tr1 cells *in vivo* 14 days p.i. (Fig 4F), providing functional support for our explanation of IL-27-mediated metabolic changes above. In addition, Th1 cells polarised from *Il27ra*^{-/-} CD4⁺ T cells were more glycolytic compared to WT Th1 cells *in vitro* (Fig 4G and S2C Fig). Previous studies reported IL-10 mediated inhibition of glycolysis in macrophages [47] and CD4⁺ T cells have been shown to respond to IL-10 signalling during *L. donovani* infection [13]. Since *Il27ra*^{-/-} CD4⁺ T cells displayed impaired IL-10 production, we examined whether this could account for the increase in glycolysis we observed. We found that the glycolytic capacity of CD4⁺ T cells from *Il27ra*^{-/-} mice was partially reduced upon the addition of IL-10 (S2D Fig). However, this did not reach statistical significance suggesting that IL-10 indirectly or only partially regulates glycolysis in CD4⁺ T cells in the absence of IL-27 signalling during *L. donovani* infection. Collectively, these data support previous work showing Th1 cells were more glycolytic than their regulatory counterparts [48], and importantly demonstrate for the first time that IL-27 signalling is an important regulator of glycolysis in Th1 cells.

IL-27 signalling limits glycolysis in Th1 cells to restrict tissue pathology

To explore the effects of increased glycolysis in Th1 cells in the absence of IL-27 signalling on disease outcomes, we infected WT and *Il27ra*^{-/-} mice with *L. donovani* and treated with either 2-DG (inhibitor of glycolysis) or PBS vehicle beginning at day 7 p.i., every day until day 14 p.i.. 2-DG treatment reduced liver weights with limited impact on parasite burdens in *Il27ra*^{-/-} mice (Fig 5A). It has previously been shown that large granulomas with diffuse foci of inflammatory infiltrates form in the liver in the absence of IL-27 signalling during *L. donovani* infection [5]. However, we found no difference in the total number of granulomas in WT and *Il27ra*^{-/-} mice at day 14 p.i. (Fig 5B and 5C), but a significant reduction in parasites (indicated by DAB staining) within the granulomas of *Il27ra*^{-/-} mice, compared to WT controls (Fig 5C), consistent with earlier parasite counts in tissue impression smears (Fig 5A). Importantly, 2-DG treatment resulted in a reduction in gross splenic pathology in *Il27ra*^{-/-} mice without impairing parasite control (Fig 5D), suggesting that increased glycolysis in the absence of IL-27 signalling may be targeted to reduce infection-induced inflammation, without impacting anti-parasitic immunity. Critically, the splenic architecture was preserved in the *Il27ra*^{-/-} mice treated with 2-DG (Fig 5E), and this was associated with reduced TNF levels in the serum (Fig 5F) and TNF production by splenic CD4⁺ T cells 14 days p.i. (Fig 5G), relative to PBS-treated *Il27ra*^{-/-} mice. In addition, we measured reduced numbers and frequencies of Th1 cells, but no effect on Tr1 cells (Fig 5H). Moreover, 2-DG had no effect on the frequencies of conventional or antigen-specific IL-10 producing Treg cells (S3A Fig). Together, these results suggest that 2-DG treatment limited Th1 cell development and function in the absence of IL-27 signalling to a level that prevented tissue damage but allowed control of parasite growth. The effects of 2-DG are not T cell specific and

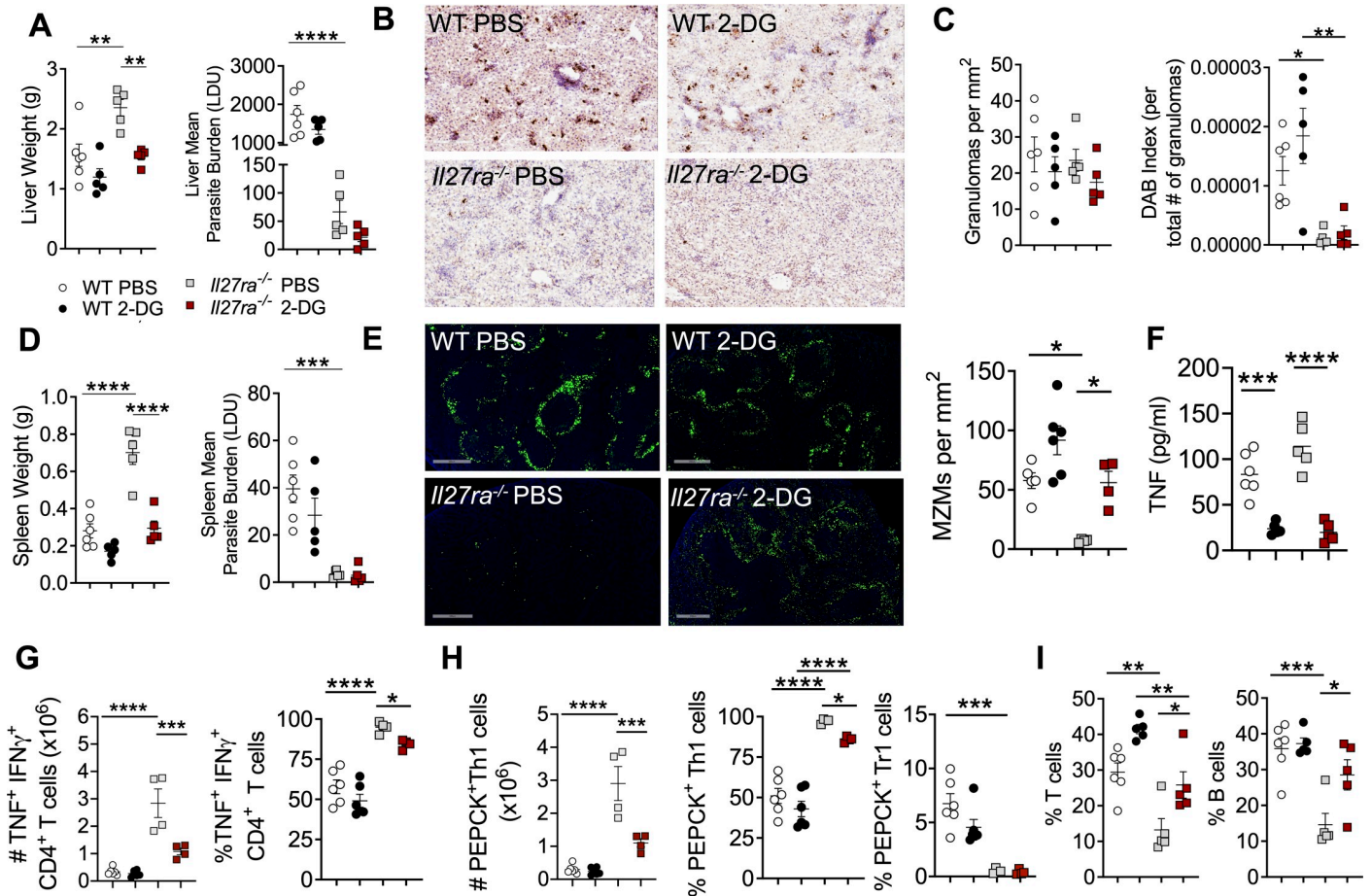


Fig 5. IL-27 signalling limits glycolysis in Th1 cells and protects against tissue pathology during infection. WT and *Il27ra*^{-/-} mice infected with 2x10⁷ *L. donovani* amastigotes i.v.. Mice were treated with PBS (controls) or 1g/kg of 2-DG daily i.p. beginning at day 7 p.i., until day 14 p.i. Organs were harvested 14 days p.i. and processed for cellular analysis. (A) Liver weights (g) and parasite burdens measured in Leishman Donovan Units (LDU: number of amastigotes per 1000 nuclei x organ weight) 14 days p.i.. (B) Liver sections (scale bars: 200µM) imaged on the Aperio XT Turbo slide scanner. (C) Total granulomas and DAB quantification (DAB index) were performed using Image J and adjusted to the section area in mm². (D) Spleen weights (g) and parasite burdens measured in LDU 14 days p.i.. (E) Marginal zone macrophages (MZMs) were quantified in the spleen by injecting mice with 100µg of FITC dextran i.v. (scale bars: 500µM) and imaged of the Aperio FL slide scanner. MZMs were quantified using Metamorph per mm². (F) TNF levels (pg/ml) measured in the serum 14 days p.i.. (G) Number and frequencies of splenic CD4⁺ T cells co-producing IFN γ and TNF was measured by flow cytometry 14 days p.i. (H) Number and frequencies of antigen-specific Th1 and Tr1 cells was measured by flow cytometry 14 days p.i. (I) T (TCR β ⁺) and B (B220⁺ CD19⁺) cell frequencies measured by flow cytometry 14 days p.i. Data shown is representative of 3 independent experiments performed with n = 4–6 mice per group, in each experiment and are presented as mean \pm SEM, ****p<0.0001, ***p<0.0005, **p<0.005, *p<0.05, One-Way ANOVA with Tukey’s multiple comparisons test.

<https://doi.org/10.1371/journal.ppat.1008994.g005>

therefore we measured other lymphocyte and myeloid populations by flow cytometry and found no obvious differences (S3B and S3C Fig). CD4⁺ T cells were the predominant source of IFN γ in all groups (S3D Fig). Collectively, these data suggest a primary effect of 2-DG in *Il27ra*^{-/-} mice on IFN γ production, and in particular on the development of Th1 cells, compared to other cell types assessed. We previously reported that IFN γ signalling was critical for induction of TNF-mediated splenic pathology and found improved lymphocyte trafficking as a result of preserved splenic architecture following TNF blockade in *L. donovani*-infected mice [12]. Indeed, the preservation of splenic architecture in the *Il27ra*^{-/-} mice treated with 2-DG resulted in increased T and B cell frequencies in this organ (Fig 5I). Taken together, these results indicate that IL-27 signalling limits glycolysis in Th1 cells *in vivo* in order to protect tissue architecture against infection-induced inflammation.

Th1 cells rely on metabolic intermediates generated during glycolysis to produce pro-inflammatory cytokines

Given 2-DG targets hexokinase at the beginning of the glycolysis pathway, we next sought to determine whether the reduced IFN γ and TNF production was a direct result of blockade of the glycolysis pathway itself or whether the administration of 2-DG was limiting the availability of metabolic intermediates for other metabolic pathways required by CD4⁺ T cells [49]. In addition to 2-DG, we used heptelicidic acid (HA) which inhibits GAPDH (Fig 6A). Interestingly, splenic Th1 cell and IFN γ ⁺ TNF⁺ CD4⁺ T cell frequencies were reduced in the 2-DG and HA treated groups (Fig 6B and 6C, S4A Fig). The same effect was also observed in the liver (Fig 6D and 6E). Collectively, these data show that IL-27 signalling limits glycolysis in Th1 cells and their ability to produce IFN γ and TNF is impaired when glycolysis and the metabolic intermediates generated from glycolysis are inhibited. Importantly, this reduction in cytokine production was directed towards Th1 cells, as we found no changes in Tr1 cell frequencies (S4B Fig).

Discussion

We previously showed that Blimp1-mediated IL-10 production by CD4⁺ T cells protects against tissue damage in the spleen following *L. donovani* infection [12]. Here we show that IL-27 signalling plays a pivotal role in generating Tr1 cells during infection, whereby *Il27ra*^{-/-}

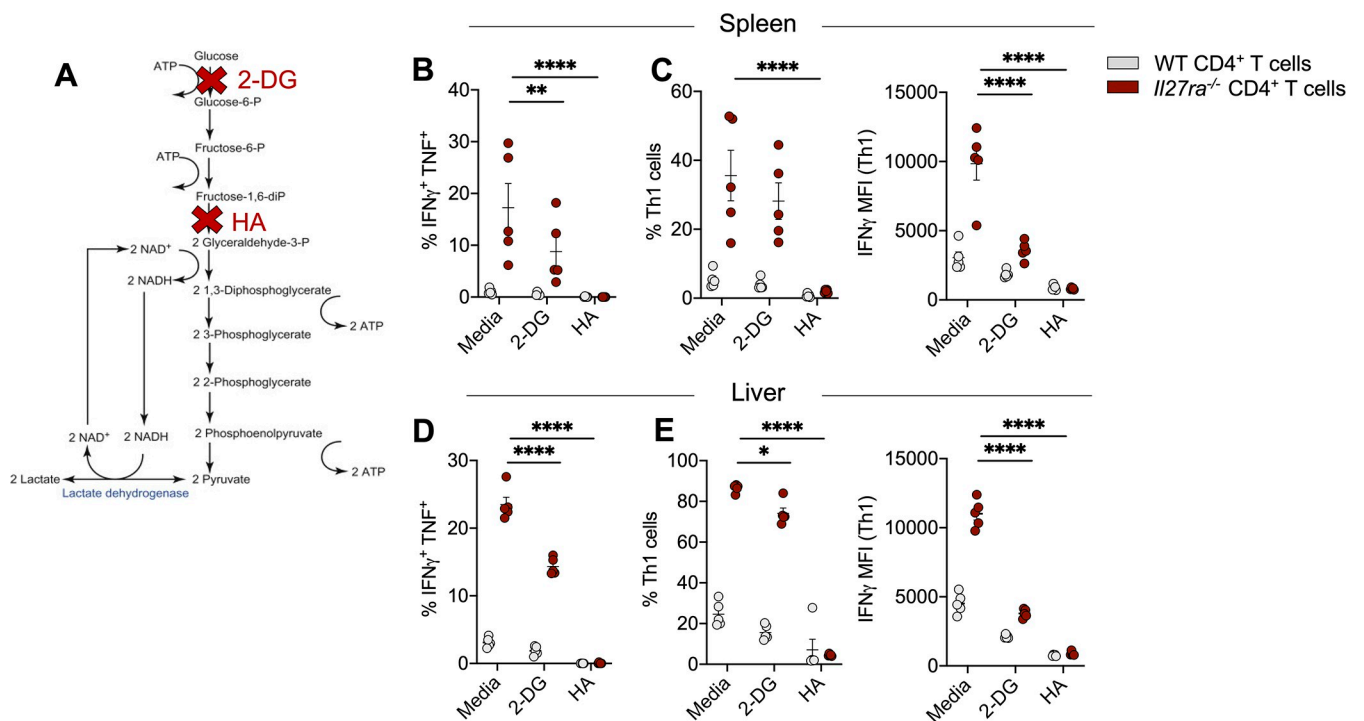


Fig 6. Th1 cells rely on metabolic intermediates generated during glycolysis to produce pro-inflammatory cytokines. (A) 2×10^5 CD4⁺ T cells were MACS purified from the spleens and livers of *L. donovani* infected WT and *Il27ra*^{-/-} mice at day 14 p.i. and treated with either media, or 1mM of either 2-DG or heptelicidic acid (HA) for 1 hour and re-stimulated with PMA/Ionomycin in the presence of monensin for 3 hours. Red crosses show the targets of 2-DG and HA within the glycolysis pathway. (B) Frequencies of IFN γ ⁺ TNF⁺ CD4⁺ T cells measured in the spleen by flow cytometry. (C) IFN γ ⁺ Tbet⁺ (Th1) cell frequencies measured in the spleen and IFN γ expression shown as the Mean Fluorescence Intensity (MFI). (D) Frequencies of IFN γ ⁺ TNF⁺ CD4⁺ T cells measured in the liver by flow cytometry. (E) IFN γ ⁺ Tbet⁺ (Th1) cell frequencies measured in the liver and IFN γ expression shown as the Mean Fluorescence Intensity (MFI). Data shown is representative of 2 independent experiments performed with $n = 5$ mice per group, in each experiment and are presented as mean \pm SEM, **** $p < 0.0001$, ** $p < 0.005$, * $p < 0.05$, Two-Way ANOVA with Sidak's multiple comparisons test.

<https://doi.org/10.1371/journal.ppat.1008994.g006>

mice had improved parasite control but accelerated splenic pathology, associated with an increased proportion of Th1 cells, relative to Tr1 cells. These findings along with others [14,20,50] highlight the importance of IL-27 signalling in regulating T cell responses during infection to protect host tissue. Here we show early MZM loss in *Il27ra*^{-/-} mice suggesting IL-27 signalling protects against IFN γ - and TNF-mediated pathology. IL-27 can exert its anti-inflammatory effects via suppression of IL-17 [14,23,31,51,52] and stimulation of IL-10 production [14,15,23,24,53–55]. These latter studies support our findings of reduced IL-10 production and Tr1 cell frequencies in the *Il27ra*^{-/-} mice.

Th1 cells are important for controlling many intracellular pathogens [56,57]. However, excess inflammation contributed by these cells can damage tissue and promote dysfunctional immune responses (reviewed in [19]). IL-27 signalling and its role in limiting Th1 cell-mediated inflammation has been reported in many experimental settings, including, encephalomyelitis [58], inflammatory bowel disease [59], tuberculosis [60], trypanosomiasis [61], malaria [20] and leishmaniasis [5]. IL-27 signalling is thought to limit the formation of pathogenic Th1 cells by suppressing CCR5 [62] and IL-2 [63,64] expression. Although IL-12-mediated IL-10 induction contributes to these effects [12,65], the mechanism underpinning this immunoregulatory axis remains unclear. Moreover, a role for Th17 cells cannot be excluded, however we were not able to detect IL-17 production by CD4⁺ T cells in the context of *Il27ra*-deficiency in this infection model.

TCR signalling increases the import of glucose and glutamine which promotes effector T cell differentiation [34,66,67]. Activated T cells preferentially use glycolysis for proliferation and to maintain effector function [34,66,67]. Additionally, mitochondrial ROS is critical for activation of NFAT and subsequent IL-2 production in T cells [45]. Consistent with these findings, we observed an increase in mitochondrial derived ROS in CD4⁺ T cells from *Il27ra*^{-/-} mice, indicative of their highly activated state, also supported by increased cell size and granularity. We hypothesised that IL-27 signalling limited glycolysis in CD4⁺ T cells as a means to prevent the hyper-activation, including excessive IFN γ and TNF production [68]. As previously reported, we also observed Th1 cells to be more glycolytic than their regulatory counterparts [48]. Recently, IL-27 and IL-15 signalling was shown to be critical for vaccine-elicited T cell responses, rather than infectious challenge [69]. CD8⁺ T cells responding to vaccination preferentially relied on mitochondrial function rather than aerobic glycolysis to support proliferation [69]. In support of these results we also show reduced IFN γ and TNF production by CD4⁺ T cells with 2-DG administration in a different infectious setting *in vivo*. Additionally, we noted decreased Th1 cell frequencies along with reduced IFN γ expression, suggesting IL-27 signalling limits glycolysis which is required for Th1 cell effector function [34].

The splenic architecture plays a crucial role in orchestrating and directing the trafficking of lymphocytes [70]. During VL, the breakdown of the splenic architecture is mediated by IFN γ and TNF [12,39], and comprises compartment-specific remodelling [71], as well as neovascularisation mediated by Ntkr2 [72]. Consistent with these findings [12], we showed glycolysis blockade in *Il27ra*^{-/-} mice rescued splenic architecture by preserving marginal zone macrophages, reducing IFN γ and TNF levels and retaining T and B cells in the spleen.

The breakdown of glucose into pyruvate during glycolysis provides metabolic intermediates that enter other metabolic pathways in order to contribute to amino acid synthesis and cell growth [73]. Our findings presented here, show that in the absence of IL-27 signalling, Th1 cells and their ability to produce IFN γ and TNF is impaired in the presence of 2-DG or heptelic acid. Hence, inhibition of the first and middle steps of glycolysis results in reduced cytokine production by *bona fide* Th1 cells during infection and had no impact on Tr1 cells, suggesting that IL-27 signalling regulates glycolysis specifically in Th1 cells. Blocking glycolysis can reduce disease severity in inflammatory environments such as those found in arthritis

[74,75], cancer [76], autoimmunity [77] and infections [48]. Our findings presented here highlight the importance of understanding the metabolic changes that occur during inflammation and how these pathways could potentially be targeted to restore functionality to tissues affected by inflammatory-mediated damage.

In conclusion, inflammation is a natural process that serves to protect the host against pathogens. Excess inflammation in the absence of appropriate immune regulation leads to a myriad of inflammatory diseases such as rheumatoid arthritis, colitis and multiple sclerosis. IL-27 signalling has been identified as a context-dependent modulator of inflammation in various settings. Here, we provide evidence for how IL-27 signalling limits Th1 cell-mediated host tissue damage by regulating glycolysis selectively in these cells. If left untreated, many inflammatory diseases progress to a chronic state resulting in dysfunctional immune responses and further host tissue damage. We show that targeting glycolysis provides an opportunity to dampen inflammation and rescues host tissue damage without compromising anti-parasitic immunity.

Materials and methods

Ethics statement

All animal procedures were approved by the QIMR Berghofer Medical Research Institute Animal Ethics Committee. This work was conducted under QIMR Berghofer animal ethics approval number A1707615M, in accordance with the “Australian Code of Practice for the Care and Use of Animals for Scientific Purposes” (Australian National Health and Medical Research Council).

Mice

Female mice aged between 8–12 weeks were used for all experiments unless stated otherwise. C57BL/6J female mice aged 8–12 weeks were purchased from the Australian Resource Centre (Canning Vale, WA, Australia). All mice were maintained under pathogen-free conditions at the QIMR Berghofer Medical Research Institute Animal Facility (Herston, QLD, Australia). Mice were bred in-house including: C57BL/6N (C57BL/6N, RRID: IMSR_JAX:005304), B6.N.129P2-*Il27ra*^{tm1Mak}/J (*Il27ra*^{-/-}, RRID: IMSR_JAX:018078)[78], B6.129S7-Rag1^{tm1Mom}/J (*Rag1*^{-/-}, RRID: IMSR_JAX:002216)[79], B6.129S6-*Il10*^{tm1Flv}/J (*Il10* GFP, RRID: IMSR_JAX:008379)[80], C57BL/6-*Foxp3*^{tm1Flv}/J (*Foxp3*RFP, RRID: IMSR_JAX:008374)[81] and B6.129S4-*Ifng*^{tm3.1Lky}/J (*Ifng*YFP, RRID: IMSR_JAX: 017581)[82].

Parasites and infections

Leishmania donovani (clone LV9) [83] parasites were maintained by *in vivo* passage in *Rag1*^{-/-} mice and amastigotes were isolated from the spleens of chronically infected mice. Mice were infected with 2×10^7 *L. donovani* amastigotes intravenously (i.v.) via the lateral tail vein. Spleen and liver impression smears were used to determine mean parasite burdens and expressed as Leishman Donovan Units (LDU = number of amastigotes per 1000 host nuclei multiplied by the organ weight in grams).

In vitro infection

Peritoneal cells were collected from WT and *Il27ra*^{-/-} mice by peritoneal lavage and washed with complete DMEM (10% v/v FCS containing 10mM L-glutamine, 100U/mL penicillin and 100mg/ml streptomycin). 5×10^5 cells were seeded in a 8-well glass chamber slide (NUN15491, Lab Tek, Thermo Fisher Scientific Australia Pty Ltd, Scoresby, VIC, Australia). After 24 hours, non-adherent cells were washed and removed with complete DMEM and 10 *L. donovani*

amastigotes per cell (MOI = 10:1) was added and incubated for 1 hour at 37°C. After 1 hour, macrophages were washed and free amastigotes removed. Cells were cultured for another 24 hours with or without 25ng/mL of recombinant IFN γ (505812, BioLegend, California, USA) or 100ng/ml recombinant IL-27 (577404, BioLegend, California, USA). The following day, cells were washed with 1x dPBS, fixed in 95% (v/v) methanol and stained using 10% (v/v) Giemsa stain (GS500, Sigma Aldrich, NSW, Australia) diluted in water. The number of parasites or number of infected cells per 100 host macrophages was measured.

***L. donovani* antigen re-stimulation assay**

Spleens were harvested and processed through a 100 μ m cell strainer to obtain a single cell suspension. Splenocyte cell suspensions were then counted and adjusted to a concentration of 2x10⁶ cells/mL. *L. donovani* amastigotes (fixed in 4% PFA) were thawed and washed in RPMI media containing Penicillin-Streptomycin and then counted and adjusted to a final concentration of 4x10⁷/ml. Cells and parasites were plated into a 96-U bottom well plate at a 1:20 ratio, where each well contained 1x10⁵ cells and 2x10⁶ parasites. Cells were then cultured with the fixed *L. donovani* amastigotes for 24–72 hours. Culture supernatants were harvested at 24 and 72 hours post culture.

Fluorescence microscopy

Mice were injected with 100 μ g i.v. of FITC dextran (D7137, Life Technologies Australia Pty Ltd, VIC, Australia), one day prior to collection of organs. Spleen tissue was collected into 4% (w/v) PFA (in PBS), incubated at room temperature for 1–2 hours and then transferred to a 30% (w/v) sucrose solution (in MilliQ water) overnight at 4°C. Fixed spleen tissue was then dabbed on filter paper to remove excess sucrose and subsequently snap frozen in O.C.T compound medium for cryotomy (00411243, Bio-strategy, Tingalpa, QLD, Australia). Splenic architecture and distribution of marginal zone macrophages (MZMs) were analysed in 20 μ m sections counter-stained with DAPI and visualised on the Aperio FL slide scanner. Image analysis was performed using Image Scope to determine area of the sections and Metamorph 7.8 (Integrated Morphometry analysis tool) (Molecular Devices, CA, USA) to count the number of MZMs per mm².

Cell processing for flow cytometry

Spleen and liver mononuclear cells were prepared for flow cytometric analysis by disassociating the tissue through a 100 μ m cell strainer or metal mesh. Single cell suspensions were then treated with RBC Lysis Buffer (R7757-100ML, Sigma Aldrich, NSW, Australia) for 7 minutes at room temperature to lyse red blood cells in each sample. Single cell suspensions were then centrifuged at 1300 rpm for 6 minutes and supernatant was decanted. Cell pellet was resuspended in 5ml of 1% FCS (in PBS) and cell viability was determined using trypan blue exclusion dye (C10228, Thermo Fisher Scientific Australia Pty Ltd, Scoresby, VIC, Australia). 2–5x10⁶ cells per well were plated in a 200 μ l volume in a 96 U-bottom well plate. Dead cells were excluded from the analysis using LIVE/DEAD fixable Aqua stain (423102, BioLegend, California, USA), as per manufacturer's instructions. For detection of intracellular cytokines, cells were re-stimulated with 25ng/ml of PMA (P8139-1MG, Sigma Aldrich, NSW, Australia), 2 μ g/ml of Ionomycin (I0634-1MG, Sigma Aldrich, NSW, Australia) in the presence of 10 μ g/mL of Brefeldin A (B6542-5MG, Sigma Aldrich, NSW, Australia) for 3 hours at 37°C. Staining for cell surface markers was performed by incubating cells with cell surface antibodies for 30 minutes at 37°C and subsequently washing with FACS buffer. Intracellular cytokine staining was then performed by permeabilising the cells with the Foxp3 Transcription Buffer Staining kit

(00-5523-00, Thermo Fisher Scientific Australia Pty Ltd, Scoresby, VIC, Australia), as per manufacturer's instructions. Cells were then resuspended in 100 μ l of FACS buffer and acquired on a BD LSR Fortessa 5 (Special order research product, BD Biosciences, Macquarie Park, NSW, Australia).

Flow cytometry

Mouse monoclonal antibodies: FITC-conjugated anti-CD11a (clone M17/4), PeCy7-conjugated anti-CD49d (clone R1-2), FITC or APC-conjugated anti-Foxp3 (clone MF-14), AF700 conjugated or BV785 conjugated anti-CD8a (clone 53-5.8), PerCP/Cy5.5 conjugated anti-CD11b (clone M1/70), PeCy7-conjugated anti-Ly6C (clone HK1.4), APC/Cy7 conjugated anti-Ly6G (clone 1A8), APC-conjugated anti-CD11c (clone N418), Pacific Blue-conjugated anti-MHCII (clone M5.114-15.3), BV650-conjugated anti-B220 (clone RA3-6B2), APC/Cy7 conjugated anti-NK1.1 (clone PK136), PE-conjugated anti-F4/80 (clone RMT4-54), PE/dazzle-conjugated anti-IL-10 (clone JES5-16E3), PeCy7 conjugated anti-Tbet (clone 4B10), APC-conjugated anti-IFN γ (clone XMG1.2), PE-conjugated anti-TNF (clone MP6-XT22) and PE-conjugated anti-IL-27p28 (clone MM27-7B1) were purchased from BioLegend (BioLegend, California, USA). BUV395-conjugated anti-CD4 (clone GK1.5) and BUV737-conjugated anti-TCR β chain (clone H57-597) were purchased from BD Biosciences (BD Biosciences, NSW, Australia). Efluor660-conjugated anti-Tbet (clone ebio4B10) was purchased from eBioscience (Thermo Fisher Scientific Australia Pty Ltd, Scoresby, VIC, Australia). I-A^b-PEPCK₃₃₅₋₃₅₁ APC tetramer [38] was obtained from the NIH, Core tetramer facility (Emory University, Atlanta, GA, USA).

Measurement of cytokine levels in the serum and/or cell culture supernatants

Cytokine levels in the serum and culture supernatants were measured using BD CBA, as per manufacturer's instructions using the mouse inflammation kit (552364, BD Biosciences, Macquarie Park, NSW, Australia). Briefly, standards were prepared by serial dilutions (0-5000pg/mL) and subsequently the master mix containing antibody-coated beads along with the detection reagent (PE) was plated into a 96 V-bottom well-plate and standards and serum or supernatant samples were added and incubated in the master mix for 2 hours at room temperature. Samples were then washed with the 1x CBA washing buffer and resuspended in a final volume of 80 μ L of wash buffer before being acquired on the HTS system plate reader on the Fortessa 5 (Special order research product, BD Biosciences, Macquarie Park, NSW, Australia). Analysis was performed using the FCAP Array v3.0 software (Soft Flow, Minnesota, USA).

Th1 cell *in vitro* polarisation

100 μ L of 5 μ g/mL Ultra-LEAF purified anti-mouse CD3 ϵ (100340; clone 145-2C11; BioLegend, California, USA), diluted in 1x dPBS (Gibco) was added to each well (except media only controls) of a 96 U-well bottom plate and incubated for 2 hours in a 37°C incubator to coat the wells. Mouse T cell media was prepared under sterile conditions and filtered, 10% FBS (Gibco), 0.05mM β -mercaptoethanol (Sigma Aldrich, NSW, Australia), 1x non-essential amino acids (Gibco), 100U/mL penicillin and 100 μ g/mL streptomycin (penicillin-streptomycin, Gibco), in Dulbecco's Modified Eagle Medium containing 4.5g/L D-Glucose, L-Glutamine and 1mM sodium pyruvate (Gibco). Media was allowed to reach 37°C prior to use. After coating, the purified anti-mouse CD3 ϵ was discarded and 100 μ L of a 2x polarisation cocktail, prepared in mouse T cell media, was added to each respective well. Briefly, media only well contained, 100 μ L of mouse T cell media, as described above. Th0 conditions contained, 2 μ g/

mL of Ultra-LEAF purified anti-mouse CD28 (102116; clone 37.51; BioLegend, California, USA) and 20ng/mL of recombinant mouse IL-2 (575404, BioLegend, California, USA). Th1 conditions contained, 2 μ g/mL of anti-mouse CD28 (102102; clone 37.51; BioLegend, California, USA), 20ng/mL of recombinant mouse IL-2 (575404, BioLegend, California, USA), 10 μ g/mL of anti-IL-4 (504122, clone 11B11, BioLegend, California, USA) and 10ng/mL of recombinant mouse IL-12p70 (577004, BioLegend, California, USA). After 72 hours, efficiency of polarisation was assessed by measuring Tbet, IFN γ , L-10 and Foxp3 expression by flow cytometry (please see [S2C Fig](#))

Assessment of cellular metabolism

3-4 $\times 10^5$ CD4⁺ T cells were plated per well and immobilised by coating plates with 0.6 μ g Corning Cell Tak adhesive (354240, In Vitro Technologies Inc., QLD, Australia) or 1 μ g Poly-D-lysine (P6407, Sigma Aldrich, NSW, Australia) prior to running the Glycolysis stress test assay (SEA103020100, In Vitro Technologies Inc., QLD, Australia) as per manufacturer's instructions. XF Base medium (SEA103335100, In Vitro Technologies Inc., QLD, Australia), supplemented with 1mM L-Glutamine (G7513, Sigma Aldrich, NSW, Australia) was prepared fresh on the day and pH adjusted to 7.4 at 37°C. For [Fig 4G](#), 100ng/mL of recombinant mouse IL-10 (575806, BioLegend, California, USA) was added to port A, glucose to port B, oligomycin to port C and 2-DG to port D.

MitoTracker staining

200nM of MitoTracker Green (M7514), 200nM MitoTracker Deep Red (M22426) (Life Technologies Australia Pty Ltd, VIC, Australia) and 5 μ M of MitoSOX Red (M36008) (Life Technologies Australia Pty Ltd, VIC, Australia) were used to identify mitochondria and mROS by flow cytometry. Cells were incubated with MitoTracker dyes for 30 mins at 37°C and then washed with HBSS (14175-103, Life Technologies Australia Pty Ltd, VIC, Australia) and then acquired on a BD FSR Fortessa 5 (BD Biosciences; special order research product).

In vivo 2-DG administration

Mice were injected with either PBS (controls) or 2-DG i.p. (D6134, Sigma Aldrich, NSW, Australia) at a dose of 1g/kg every for 7 days, beginning at day 7 p.i. until day 14 p.i.

In vitro glycolysis blockade

Spleens and livers were harvested from WT and *Il27ra*^{-/-} mice 14 days p.i. and CD4⁺ T cells were MACS purified as above. 2 $\times 10^5$ CD4⁺ T cells were plated out in combination with media or 1mM of either 2-DG (D6134, Sigma Aldrich, NSW, Australia) or heptelidic acid (14079, Sapphire Bioscience Pty Ltd, NSW, Australia) and incubated at 37°C for 1 hour and then restimulated with 25ng/ml of PMA (P8139-1MG, Sigma Aldrich, NSW, Australia), 2 μ g/ml of Ionomycin (I0634-1MG, Sigma Aldrich, NSW, Australia) in the presence of 2 μ M of Monensin (420701, BioLegend, California, USA) for 3 hours at 37°C. CD4⁺ T cells were then stained for cell surface markers and intracellular markers, as described above and acquired on a BD LSR Fortessa 5 (BD Biosciences; special order research product).

Liver granulomas

7 μ m frozen sections were dried overnight then fixed in a 3:1 mix of anhydrous acetone/ethanol for 5 minutes. Endogenous peroxidase was blocked using 0.5% (v/v) hydrogen peroxide in methanol for 10 minutes and non-specific binding of the primary antibody minimized by

incubating sections in Biocare Medical Background Sniper plus 2.0% (w/v) BSA for 10 minutes. The primary antibody, hamster anti-mouse LV9 diluted 1:1000 in Biocare Medical Da Vinci Green antibody diluent, was applied for 60 minutes then detected by applying Jackson ImmunoResearch goat anti-hamster secondary, diluted 1:300 in TBS, for 30 minutes followed by a 30 minute application of Vector ImmPRESS Goat HRP polymer. LV9 signal was visualized using Vector ImmPACT DAB. Sections were counterstained with Mayer's Haematoxylin in a Leica Autostainer XL and mounted using a Leica CV5030 coverslipper.

Granuloma image analysis

Granulomas were imaged in Image Processing and Analysis in Java [84] (Image J, NIH, Bethesda, Maryland, USA). Images were processed with the following settings: image threshold: 155–190, details of the script modified under: Granuloma_macro_edit2.

Statistical analysis

Statistical analysis was performed using GraphPad Prism software version 7.02 (Graphpad, San Diego, CA, USA). Two independent groups were compared using a non-parametric Mann-Whitney U test, where * $p < 0.05$, ** $p < 0.01$ was considered to be statistically significant. Groups with two or more dependent variables were compared using a One-Way ANOVA with Tukey's multiple comparisons test or a Two-Way ANOVA with Sidak's multiple comparisons test, where * $p < 0.05$, ** $p < 0.005$, *** $p < 0.001$, **** $p < 0.0001$. All data are presented as the mean \pm SEM.

Supporting information

S1 Fig. IL-27 signalling regulates CD4⁺ T cell responses during *L. donovani* infection.

C57BL/6J mice were infected with 2×10^7 *L. donovani* amastigotes i.v.. Antigen (PEPCK⁺)-specific CD4⁺ T cell responses measured by flow cytometry in the (A) spleen and (B) liver 14 days p.i. Antigen-specific CD4⁺ T cells defined as Foxp3⁻CD4⁺ TCR β ⁺ CD44⁺ PEPCK⁺. From the antigen-specific CD4⁺ T cell gate, Tr1 cells defined as IL-10⁺ IFN γ ⁺ and from the IFN γ ⁺ IL-10⁻ gate, Th1 cells defined as Tbet⁺ IFN γ ⁺. Line graphs track the frequencies of antigen-specific CD4⁺ T cells throughout the course of infection including, day 0, 7, 14, 28 and 56 p.i. in the spleen (white circles) and liver (black circles). (C) WT and *Il27ra*^{-/-} mice were infected with 2×10^7 *L. donovani* amastigotes i.v.. CD4⁺ T cell frequencies defined as CD4⁺ TCR β ⁺. Antigen specific CD4⁺ T cell frequencies defined as CD44⁺ PEPCK⁺. Antigen specific Th1 cell frequencies defined as CD44⁺ PEPCK⁺ Tbet⁺ IFN γ ⁺. Antigen specific Tr1 cell frequencies defined as CD44⁺ PEPCK⁺ IL-10⁺ IFN γ ⁺. Antigen specific Treg cell frequencies defined as CD44⁺ PEPCK⁺ Foxp3⁺ IL-10⁺ by flow cytometry in the spleen and liver. (D) IFN γ , TNF and IL-10 levels (pg/mL) measured in the serum 14 days p.i. (E) WT and *Il27ra*^{-/-} mice were infected with 2×10^7 *L. donovani* amastigotes i.v. and 14 days p.i. mitochondrial volume (Vol) and membrane potential (MP) was measured on Th1 cells identified as CXCR3⁺ CXCR5⁻ (gated on CD4⁺ TCR β ⁺) by flow cytometry. (F) WT and *Il27ra*^{-/-} mice were infected with 2×10^7 *L. donovani* amastigotes i.v.. Th1 cell frequencies measured by flow cytometry in uninfected and infected mice *ex vivo* 14 days p.i. (G) Peritoneal cells were isolated from WT and *Il27ra*^{-/-} mice and incubated with *L. donovani* amastigotes for 24 hours with or without IFN γ or IL-27. Number of parasites or infected cells per 100 host macrophages are shown as a measure of infectivity. Data shown is representative of 2 independent experiments performed with $n = 4$ –6 mice per group, in each experiment and are presented as mean \pm SEM. C, D: ** $p < 0.01$, Mann-Whitney U test, F, G: **** $p < 0.0001$, *** $p < 0.0005$, ** $p < 0.005$, One-Way ANOVA with

Tukey's multiple comparisons test.
(TIF)

S2 Fig. IL-27 signalling limits glycolysis to regulate cytokine production. WT and *Il27ra*^{-/-} mice were infected with 2×10^7 *L. donovani* amastigotes i.v.. Splenic and hepatic CD4⁺ T cells were MACS purified and assayed on the Seahorse XF96 using the glycolysis stress test kit at day 14 p.i.. Total oxygen consumption rate (OCR) was assessed after the addition of glucose, oligomycin and 2-DG at indicated times in the (A) spleen and (B) liver. (C) Naïve WT splenic CD4⁺ T cells MACS purified and polarised to Th0 and Th1 conditions. 72 hours later polarisation efficiency assessed by measuring Tbet, IFN γ , IL-10 and Foxp3 expression by flow cytometry. (D) Splenic CD4⁺ T cells MACS purified from day 14 infected WT and *Il27ra*^{-/-} mice and treated with 100ng/mL of recombinant mouse IL-10 as part of the injection protocol, 30 minutes before the addition of glucose, oligomycin and 2-DG on the Seahorse XF96. Glycolytic capacity was calculated as: (Maximum rate measurement after Oligomycin injection)–(Last rate measurement before Glucose injection), Glycolysis (ECAR) measured in all conditions. Data shown is representative of 2 independent experiments performed with $n = 5-6$ mice per group, in each experiment and are presented as mean \pm SEM, *** $p < 0.0005$, One-Way ANOVA with Tukey's multiple comparisons test.
(TIF)

S3 Fig. 2-DG treatment exhibits a minor effect on immune cell populations in the spleen and CD4⁺ T cells are the predominant source of IFN γ . WT and *Il27ra*^{-/-} mice infected with 2×10^7 *L. donovani* amastigotes i.v.. Mice were treated with PBS (controls) or 1g/kg of 2-DG daily i.p. beginning at day 7 p.i. until day 14 p.i. Organs were harvested 14 days p.i. and processed for cellular analysis. (A) Conventional and antigen-specific Tregs producing IL-10 were measured by flow cytometry 14 days p.i. (B) Gating strategy for CD4⁺ T cells (red), CD8⁺ T cells (blue), NK1.1⁺ (green), CD19⁺ (orange), CD11c⁺ (yellow), CD11b⁺ (purple), Ly6C⁺ (teal), Ly6G⁺ (pink), F4/80⁺ dextran⁺ (grey) cells were analysed by flow cytometry in the spleen 14 days p.i. (C) Frequencies and numbers of CD4⁺ T cells, CD8⁺ T cells, NK1.1⁺, CD19⁺, CD11c⁺, CD11b⁺, Ly6C⁺, Ly6G⁺, F4/80⁺ dextran⁺ cells were analysed by flow cytometry in the spleen 14 days p.i. (D) Cellular sources of IFN γ was measured by flow cytometry in the spleen 14 days p.i. same gating strategy as described in B, but gating on total IFN γ ⁺ events after the live/dead gate. Data shown is representative of 3 independent experiments performed with $n = 4-6$ mice per group, in each experiment and are presented as mean \pm SEM, ** $p < 0.005$, One-Way ANOVA with Tukey's multiple comparisons test.
(TIF)

S4 Fig. IL-27 signalling limits glycolysis to regulate cytokine production by Th1 cells and not Tr1 cells. (A) 2×10^5 CD4⁺ T cells were MACS purified from the spleens and livers of WT and *Il27ra*^{-/-} mice at day 14 p.i. and treated with either media, or 1mM of either 2-DG or heptelic acid (HA) for 1 hour and re-stimulated with PMA/Ionomycin in the presence of monensin for 3 hours. Th1 (Tbet⁺ IFN γ ⁺) cell frequencies were measured by flow cytometry. Plots for Tbet (x-axis) and IFN γ (y-axis) are shown for each treatment. (B) Tr1 (IL-10⁺ IFN γ ⁺) cell frequencies shown in response to media, 2-DG and HA treatment, as described in S4A Fig. Data shown is representative of 2 independent experiments performed with $n = 5$ mice per group, in each experiment and are presented as mean \pm SEM, * $p < 0.05$, Two-Way ANOVA with Sidak's multiple comparisons test.
(TIF)

Acknowledgments

We gratefully acknowledge the assistance of the QIMR Berghofer flow cytometry facility, animal facilities and the histology and microscopy facilities. We thank Tam Hong Nguyen and Nigel Waterhouse for their assistance in image analysis, Sang-Hee Park for sectioning spleen tissue samples and Andrew Masel for his assistance with histological services. We thank the NIH tetramer facility (Atlanta, GA) for production of the I-A^b-PEPCK₃₃₅₋₃₅₁ tetramer used to detect *L. donovani* PEPCK-specific CD4⁺ T cells in these studies.

Author Contributions

Conceptualization: Marcela Montes de Oca, Agnieszka Kabat, Ramon I. Klein Geltink, Edward J. Pearce, Geoffrey R. Hill, Christian R. Engwerda.

Data curation: Marcela Montes de Oca, Fabian de Labastida Rivera, Clay Winterford, Teija C. M. Frame, Susanna S. Ng, Christian R. Engwerda.

Formal analysis: Marcela Montes de Oca, Fabian de Labastida Rivera, Clay Winterford, Teija C. M. Frame, Susanna S. Ng, Fiona H. Amante, Chelsea L. Edwards, Luzia Bukali, Yulin Wang, Rachel D. Kuns, Ping Zhang, Agnieszka Kabat, Ramon I. Klein Geltink, Christian R. Engwerda.

Funding acquisition: Marcela Montes de Oca, Edward J. Pearce, Christian R. Engwerda.

Investigation: Marcela Montes de Oca, Fabian de Labastida Rivera, Clay Winterford, Teija C. M. Frame, Susanna S. Ng, Fiona H. Amante, Chelsea L. Edwards, Luzia Bukali, Yulin Wang, Rachel D. Kuns, Ping Zhang, Agnieszka Kabat, Ramon I. Klein Geltink.

Methodology: Marcela Montes de Oca, Fabian de Labastida Rivera, Clay Winterford, Jude E. Uzonna, Rachel D. Kuns, Ping Zhang, Agnieszka Kabat, Ramon I. Klein Geltink, Edward J. Pearce.

Project administration: Marcela Montes de Oca, Christian R. Engwerda.

Resources: Clay Winterford, Jude E. Uzonna, Rachel D. Kuns, Ping Zhang, Geoffrey R. Hill.

Supervision: Marcela Montes de Oca, Edward J. Pearce, Geoffrey R. Hill, Christian R. Engwerda.

Validation: Marcela Montes de Oca, Fabian de Labastida Rivera, Clay Winterford, Teija C. M. Frame, Susanna S. Ng, Christian R. Engwerda.

Visualization: Marcela Montes de Oca, Christian R. Engwerda.

Writing – original draft: Marcela Montes de Oca, Ping Zhang, Agnieszka Kabat, Ramon I. Klein Geltink, Edward J. Pearce, Geoffrey R. Hill, Christian R. Engwerda.

Writing – review & editing: Marcela Montes de Oca, Ping Zhang, Agnieszka Kabat, Ramon I. Klein Geltink, Edward J. Pearce, Geoffrey R. Hill, Christian R. Engwerda.

References

1. Singh OP, Gidwani K, Kumar R, Nysten S, Jones SL, Boelaert M, et al. Reassessment of immune correlates in human visceral leishmaniasis as defined by cytokine release in whole blood. *Clinical and vaccine immunology: CVI*. 2012; 19(6):961–6. <https://doi.org/10.1128/CVI.00143-12> PMID: 22539471
2. Costa CH, Werneck GL, Costa DL, Holanda TA, Aguiar GB, Carvalho AS, et al. Is severe visceral leishmaniasis a systemic inflammatory response syndrome? A case control study. *Revista da Sociedade Brasileira de Medicina Tropical*. 2010; 43(4):386–92. <https://doi.org/10.1590/s0037-86822010000400010> PMID: 20802936

3. Herwaldt BL. Leishmaniasis. *Lancet* (London, England). 1999; 354(9185):1191–9.
4. Burza S, Croft SL, Boelaert M. Leishmaniasis. *The Lancet*. 2018; 392(10151):951–70.
5. Rosas LE, Satoskar AA, Roth KM, Keiser TL, Barbi J, Hunter C, et al. Interleukin-27R (WSX-1/T-Cell Cytokine Receptor) Gene-Deficient Mice Display Enhanced Resistance to *Leishmania donovani* Infection but Develop Severe Liver Immunopathology. *The American Journal of Pathology*. 2006; 168(1):158–69. <https://doi.org/10.2353/ajpath.2006.050013> PMID: 16400019
6. Smelt SC, Engwerda CR, McCrossen M, Kaye PM. Destruction of follicular dendritic cells during chronic visceral leishmaniasis. *Journal of immunology* (Baltimore, Md: 1950). 1997; 158(8):3813–21.
7. Wilson ME, Sandor M, Blum AM, Young BM, Metwali A, Elliott D, et al. Local suppression of IFN-gamma in hepatic granulomas correlates with tissue-specific replication of *Leishmania chagasi*. *Journal of immunology* (Baltimore, Md: 1950). 1996; 156(6):2231–9.
8. Medzhitov R. Origin and physiological roles of inflammation. *Nature*. 2008; 454(7203):428–35. <https://doi.org/10.1038/nature07201> PMID: 18650913
9. Kominsky DJ, Campbell EL, Colgan SP. Metabolic shifts in immunity and inflammation. *Journal of immunology* (Baltimore, Md: 1950). 2010; 184(8):4062–8.
10. Kaye PM, Svensson M, Ato M, Maroof A, Polley R, Stager S, et al. The immunopathology of experimental visceral leishmaniasis. *Immunol Rev*. 2004; 201:239–53. <https://doi.org/10.1111/j.0105-2896.2004.00188.x> PMID: 15361245
11. Stanley AC, Engwerda CR. Balancing immunity and pathology in visceral leishmaniasis. *Immunol Cell Biol*. 2007; 85(2):138–47. <https://doi.org/10.1038/sj.icb.7100011> PMID: 17146466
12. Montes de Oca M, Kumar R, de Labastida Rivera F, Amante FH, Sheel M, Faleiro RJ, et al. Blimp-1-Dependent IL-10 Production by Tr1 Cells Regulates TNF-Mediated Tissue Pathology. *PLOS Pathogens*. 2016; 12(1):e1005398. <https://doi.org/10.1371/journal.ppat.1005398> PMID: 26765224
13. Bunn PT, Montes de Oca M, de Labastida Rivera F, Kumar R, Ng SS, Edwards CL, et al. Distinct Roles for CD4(+) Foxp3(+) Regulatory T Cells and IL-10-Mediated Immunoregulatory Mechanisms during Experimental Visceral Leishmaniasis Caused by *Leishmania donovani*. *Journal of immunology* (Baltimore, Md: 1950). 2018; 201(11):3362–72.
14. Anderson CF, Stumhofer JS, Hunter CA, Sacks D. IL-27 regulates IL-10 and IL-17 from CD4+ cells in nonhealing *Leishmania major* infection. *Journal of immunology* (Baltimore, Md: 1950). 2009; 183(7):4619–27.
15. Ansari NA, Kumar R, Gautam S, Nylén S, Singh OP, Sundar S, et al. IL-27 and IL-21 are associated with T cell IL-10 responses in human visceral leishmaniasis. *Journal of immunology* (Baltimore, Md: 1950). 2011; 186(7):3977–85.
16. Apetoh L, Quintana FJ, Pot C, Joller N, Xiao S, Kumar D, et al. The aryl hydrocarbon receptor interacts with c-Maf to promote the differentiation of type 1 regulatory T cells induced by IL-27. *Nature Immunology*. 2010; 11:854. <https://doi.org/10.1038/ni.1912> PMID: 20676095
17. Awasthi A, Carrier Y, Peron JPS, Bettelli E, Kamanaka M, Flavell RA, et al. A dominant function for interleukin 27 in generating interleukin 10–producing anti-inflammatory T cells. *Nature Immunology*. 2007; 8:1380. <https://doi.org/10.1038/ni1541> PMID: 17994022
18. Chihara N, Madi A, Kondo T, Zhang H, Acharya N, Singer M, et al. Induction and transcriptional regulation of the co-inhibitory gene module in T cells. *Nature*. 2018; 558(7710):454–9. <https://doi.org/10.1038/s41586-018-0206-z> PMID: 29899446
19. Engwerda CR, Ng SS, Bunn PT. The Regulation of CD4+ T Cell Responses during Protozoan Infections. *Frontiers in Immunology*. 2014; 5(498).
20. Findlay EG, Greig R, Stumhofer JS, Hafalla JCR, de Souza JB, Saris CJ, et al. Essential Role for IL-27 Receptor Signaling in Prevention of Th1-Mediated Immunopathology during Malaria Infection. *The Journal of Immunology*. 2010; 185(4):2482. <https://doi.org/10.4049/jimmunol.0904019> PMID: 20631310
21. Karwacz K, Miraldi ER, Pokrovskii M, Madi A, Yosef N, Wortman I, et al. Critical role of IRF1 and BATF in forming chromatin landscape during type 1 regulatory cell differentiation. *Nat Immunol*. 2017; 18(4):412–21. <https://doi.org/10.1038/ni.3683> PMID: 28166218
22. Mascanfroni ID, Takenaka MC, Yeste A, Patel B, Wu Y, Kenison JE, et al. Metabolic control of type 1 regulatory T cell differentiation by AHR and HIF1- α . *Nature medicine*. 2015; 21:638. <https://doi.org/10.1038/nm.3868> PMID: 26005855
23. Murugaiyan G, Mittal A, Lopez-Diego R, Maier LM, Anderson DE, Weiner HL. IL-27 Is a Key Regulator of IL-10 and IL-17 Production by Human CD4⁺ T Cells. *The Journal of Immunology*. 2009; 183(4):2435. <https://doi.org/10.4049/jimmunol.0900568> PMID: 19625647
24. Pot C, Jin H, Awasthi A, Liu SM, Lai C-Y, Madan R, et al. Cutting Edge: IL-27 Induces the Transcription Factor c-Maf, Cytokine IL-21, and the Costimulatory Receptor ICOS that Coordinately Act Together to

- Promote Differentiation of IL-10-Producing Tr1 Cells. *The Journal of Immunology*. 2009; 183(2):797. <https://doi.org/10.4049/jimmunol.0901233> PMID: 19570826
25. Belle L, Agle K, Zhou V, Yin-Yuan C, Komorowski R, Eastwood D, et al. Blockade of interleukin-27 signaling reduces GVHD in mice by augmenting Treg reconstitution and stabilizing Foxp3 expression. *Blood*. 2016; 128(16):2068–82. <https://doi.org/10.1182/blood-2016-02-698241> PMID: 27488350
 26. Pflanz S, Timans JC, Cheung J, Rosales R, Kanzler H, Gilbert J, et al. IL-27, a heterodimeric cytokine composed of EBI3 and p28 protein, induces proliferation of naive CD4+ T cells. *Immunity*. 2002; 16(6):779–90. [https://doi.org/10.1016/s1074-7613\(02\)00324-2](https://doi.org/10.1016/s1074-7613(02)00324-2) PMID: 12121660
 27. Pflanz S, Hibbert L, Mattson J, Rosales R, Vaisberg E, Bazan JF, et al. WSX-1 and glycoprotein 130 constitute a signal-transducing receptor for IL-27. *Journal of immunology (Baltimore, Md: 1950)*. 2004; 172(4):2225–31.
 28. Takeda A, Hamano S, Yamanaka A, Hanada T, Ishibashi T, Mak TW, et al. Cutting edge: role of IL-27/WSX-1 signaling for induction of T-bet through activation of STAT1 during initial Th1 commitment. *Journal of immunology (Baltimore, Md: 1950)*. 2003; 170(10):4886–90.
 29. Kamiya S, Owaki T, Morishima N, Fukai F, Mizuguchi J, Yoshimoto T. An Indispensable Role for STAT1 in IL-27-Induced T-bet Expression but Not Proliferation of Naive CD4⁺ T Cells. *The Journal of Immunology*. 2004; 173(6):3871. <https://doi.org/10.4049/jimmunol.173.6.3871> PMID: 15356135
 30. Stumhofer JS, Silver JS, Laurence A, Porrett PM, Harris TH, Turka LA, et al. Interleukins 27 and 6 induce STAT3-mediated T cell production of interleukin 10. *Nature Immunology*. 2007; 8:1363. <https://doi.org/10.1038/ni1537> PMID: 17994025
 31. Quirino GFS, Nascimento MSL, Davoli-Ferreira M, Sacramento LA, Lima MHF, Almeida RP, et al. Interleukin-27 (IL-27) Mediates Susceptibility to Visceral Leishmaniasis by Suppressing the IL-17–Neutrophil Response. *Infection and Immunity*. 2016; 84(8):2289–98. <https://doi.org/10.1128/IAI.00283-16> PMID: 27245409
 32. dos Santos PL, de Oliveira FA, Santos MLB, Cunha LCS, Lino MTB, de Oliveira MFS, et al. The Severity of Visceral Leishmaniasis Correlates with Elevated Levels of Serum IL-6, IL-27 and sCD14. *PLOS Neglected Tropical Diseases*. 2016; 10(1):e0004375. <https://doi.org/10.1371/journal.pntd.0004375> PMID: 26814478
 33. MacIver NJ, Michalek RD, Rathmell JC. Metabolic regulation of T lymphocytes. *Annual review of immunology*. 2013; 31:259–83. <https://doi.org/10.1146/annurev-immunol-032712-095956> PMID: 23298210
 34. Michalek RD, Gerriets VA, Jacobs SR, Macintyre AN, MacIver NJ, Mason EF, et al. Cutting edge: distinct glycolytic and lipid oxidative metabolic programs are essential for effector and regulatory CD4+ T cell subsets. *Journal of immunology (Baltimore, Md: 1950)*. 2011; 186(6):3299–303.
 35. Klysz D, Tai X, Robert PA, Craveiro M, Cretenet G, Oburoglu L, et al. Glutamine-dependent alpha-ketoglutarate production regulates the balance between T helper 1 cell and regulatory T cell generation. *Science signaling*. 2015; 8(396):ra97. <https://doi.org/10.1126/scisignal.aab2610> PMID: 26420908
 36. Peng M, Yin N, Chhangawala S, Xu K, Leslie CS, Li MO. Aerobic glycolysis promotes T helper 1 cell differentiation through an epigenetic mechanism. *Science*. 2016; 354(6311):481–4. <https://doi.org/10.1126/science.aaf6284> PMID: 27708054
 37. Chang CH, Curtis JD, Maggi LB Jr., Faubert B, Villarino AV, O’Sullivan D, et al. Posttranscriptional control of T cell effector function by aerobic glycolysis. *Cell*. 2013; 153(6):1239–51. <https://doi.org/10.1016/j.cell.2013.05.016> PMID: 23746840
 38. Mou Z, Li J, Boussoffara T, Kishi H, Hamana H, Ezzati P, et al. Identification of broadly conserved cross-species protective Leishmania antigen and its responding CD4+ T cells. *Science translational medicine*. 2015; 7(310):310ra167. <https://doi.org/10.1126/scitranslmed.aac5477> PMID: 26491077
 39. Engwerda CR, Ato M, Cotterell SE, Mynott TL, Tschannerl A, Gorak-Stolinska PM, et al. A role for tumor necrosis factor-alpha in remodeling the splenic marginal zone during Leishmania donovani infection. *Am J Pathol*. 2002; 161(2):429–37. [https://doi.org/10.1016/s0002-9440\(10\)64199-5](https://doi.org/10.1016/s0002-9440(10)64199-5) PMID: 12163368
 40. Geltink RIK, Kyle RL, Pearce EL. Unraveling the Complex Interplay Between T Cell Metabolism and Function. *Annual review of immunology*. 2018; 36:461–88. <https://doi.org/10.1146/annurev-immunol-042617-053019> PMID: 29677474
 41. Bankoti R, Stäger S. Differential Regulation of the Immune Response in the Spleen and Liver of Mice Infected with Leishmania donovani. *J Trop Med*. 2012; 2012:639304–. <https://doi.org/10.1155/2012/639304> PMID: 21811511
 42. Murray HW. Tissue granuloma structure-function in experimental visceral leishmaniasis. *Int J Exp Pathol*. 2001; 82(5):249–67. <https://doi.org/10.1046/j.1365-2613.2001.00199.x> PMID: 11703536

43. Bunn PT, Montes de Oca M, Rivera FdL, Kumar R, Edwards CL, Faleiro RJ, et al. Galectin-1 Impairs the Generation of Anti-Parasitic Th1 Cell Responses in the Liver during Experimental Visceral Leishmaniasis. *Frontiers in immunology*. 2017; 8:1307–. <https://doi.org/10.3389/fimmu.2017.01307> PMID: 29075269
44. Kaminski MM, Sauer SW, Kaminski M, Opp S, Ruppert T, Grigaravicius P, et al. T cell activation is driven by an ADP-dependent glucokinase linking enhanced glycolysis with mitochondrial reactive oxygen species generation. *Cell Rep*. 2012; 2(5):1300–15. <https://doi.org/10.1016/j.celrep.2012.10.009> PMID: 23168256
45. Sena LA, Li S, Jairaman A, Prakriya M, Ezponda T, Hildeman DA, et al. Mitochondria are required for antigen-specific T cell activation through reactive oxygen species signaling. *Immunity*. 2013; 38(2):225–36. <https://doi.org/10.1016/j.immuni.2012.10.020> PMID: 23415911
46. Bunn PT, Stanley AC, de Labastida Rivera F, Mulherin A, Sheel M, Alexander CE, et al. Tissue Requirements for Establishing Long-Term CD4+ T Cell-Mediated Immunity following *Leishmania donovani* Infection. *The Journal of Immunology*. 2014; 192(8):3709. <https://doi.org/10.4049/jimmunol.1300768> PMID: 24634490
47. Ip WKE, Hoshi N, Shouval DS, Snapper S, Medzhitov R. Anti-inflammatory effect of IL-10 mediated by metabolic reprogramming of macrophages. *Science*. 2017; 356(6337):513. <https://doi.org/10.1126/science.aal3535> PMID: 28473584
48. Varanasi SK, Donohoe D, Jaggi U, Rouse BT. Manipulating Glucose Metabolism during Different Stages of Viral Pathogenesis Can Have either Detrimental or Beneficial Effects. *The Journal of Immunology*. 2017; 199(5):1748. <https://doi.org/10.4049/jimmunol.1700472> PMID: 28768727
49. Hui S, Ghergurovich JM, Morscher RJ, Jang C, Teng X, Lu W, et al. Glucose feeds the TCA cycle via circulating lactate. *Nature*. 2017; 551:115. <https://doi.org/10.1038/nature24057> PMID: 29045397
50. Maroof A, Kaye PM. Temporal Regulation of Interleukin-12p70 (IL-12p70) and IL-12-Related Cytokines in Splenic Dendritic Cell Subsets during *Leishmania donovani* Infection. *Infection, Immunity and Immunity*. 2008; 76(1):239. <https://doi.org/10.1128/IAI.00643-07> PMID: 17998312
51. Murugaiyan G, Mittal A, Weiner HL. Identification of an IL-27/osteopontin axis in dendritic cells and its modulation by IFN-gamma limits IL-17-mediated autoimmune inflammation. *Proceedings of the National Academy of Sciences of the United States of America*. 2010; 107(25):11495–500. <https://doi.org/10.1073/pnas.1002099107> PMID: 20534530
52. Yoshimura T, Takeda A, Hamano S, Miyazaki Y, Kinjyo I, Ishibashi T, et al. Two-Sided Roles of IL-27: Induction of Th1 Differentiation on Naive CD4+ T Cells versus Suppression of Proinflammatory Cytokine Production Including IL-23-Induced IL-17 on Activated CD4+ T Cells Partially Through STAT3-Dependent Mechanism. *The Journal of Immunology*. 2006; 177(8):5377. <https://doi.org/10.4049/jimmunol.177.8.5377> PMID: 17015723
53. Shiokawa A, Tanabe K, Tsuji NM, Sato R, Hachimura S. IL-10 and IL-27 producing dendritic cells capable of enhancing IL-10 production of T cells are induced in oral tolerance. *Immunology letters*. 2009; 125(1):7–14. <https://doi.org/10.1016/j.imlet.2009.05.002> PMID: 19446579
54. Sun J, Dodd H, Moser EK, Sharma R, Braciale TJ. CD4+ T cell help and innate-derived IL-27 induce Blimp-1-dependent IL-10 production by antiviral CTLs. *Nature Immunology*. 2011; 12:327. <https://doi.org/10.1038/ni.1996> PMID: 21297642
55. Zhu C, Sakuishi K, Xiao S, Sun Z, Zaghouani S, Gu G, et al. An IL-27/NFIL3 signalling axis drives Tim-3 and IL-10 expression and T-cell dysfunction. *Nature communications*. 2015; 6:6072. <https://doi.org/10.1038/ncomms7072> PMID: 25614966
56. Reiner SL, Locksley RM. The regulation of immunity to *Leishmania major*. *Annual review of immunology*. 1995; 13:151–77. <https://doi.org/10.1146/annurev.iy.13.040195.001055> PMID: 7612219
57. Romagnani S. Understanding the role of Th1/Th2 cells in infection. *Trends in microbiology*. 1996; 4(12):470–3. [https://doi.org/10.1016/s0966-842x\(97\)82906-x](https://doi.org/10.1016/s0966-842x(97)82906-x) PMID: 9004401
58. Batten M, Li J, Yi S, Kljavin NM, Danilenko DM, Lucas S, et al. Interleukin 27 limits autoimmune encephalomyelitis by suppressing the development of interleukin 17-producing T cells. *Nature Immunology*. 2006; 7:929. <https://doi.org/10.1038/ni1375> PMID: 16906167
59. Villarino AV, Artis D, Bezbradica JS, Miller O, Saris CJM, Joyce S, et al. IL-27R deficiency delays the onset of colitis and protects from helminth-induced pathology in a model of chronic IBD. *International immunology*. 2008; 20(6):739–52. <https://doi.org/10.1093/intimm/dxn032> PMID: 18375937
60. Hölscher C, Hölscher A, Rückerl D, Yoshimoto T, Yoshida H, Mak T, et al. The IL-27 Receptor Chain WSX-1 Differentially Regulates Antibacterial Immunity and Survival during Experimental Tuberculosis. *The Journal of Immunology*. 2005; 174(6):3534. <https://doi.org/10.4049/jimmunol.174.6.3534> PMID: 15749890

61. Hamano S, Himeno K, Miyazaki Y, Ishii K, Yamanaka A, Takeda A, et al. WSX-1 Is Required for Resistance to *Trypanosoma cruzi* Infection by Regulation of Proinflammatory Cytokine Production. *Immunity*. 2003; 19(5):657–67. [https://doi.org/10.1016/s1074-7613\(03\)00298-x](https://doi.org/10.1016/s1074-7613(03)00298-x) PMID: 14614853
62. Gwyer Findlay E, Villegas-Mendez A, de Souza JB, Inkson CA, Shaw TN, Saris CJ, et al. IL-27 receptor signaling regulates CD4+ T cell chemotactic responses during infection. *Journal of immunology (Baltimore, Md: 1950)*. 2013; 190(9):4553–61.
63. Owaki T, Asakawa M, Kamiya S, Takeda K, Fukai F, Mizuguchi J, et al. IL-27 Suppresses CD28-Mediated IL-2 Production through Suppressor of Cytokine Signaling 3. *The Journal of Immunology*. 2006; 176(5):2773. <https://doi.org/10.4049/jimmunol.176.5.2773> PMID: 16493033
64. Villarino AV, Stumhofer JS, Saris CJM, Kastelein RA, de Sauvage FJ, Hunter CA. IL-27 Limits IL-2 Production during Th1 Differentiation. *The Journal of Immunology*. 2006; 176(1):237. <https://doi.org/10.4049/jimmunol.176.1.237> PMID: 16365415
65. Perona-Wright G, Mohrs K, Szaba FM, Kummer LW, Madan R, Karp CL, et al. Systemic but not local infections elicit immunosuppressive IL-10 production by natural killer cells. *Cell Host Microbe*. 2009; 6(6):503–12. <https://doi.org/10.1016/j.chom.2009.11.003> PMID: 20006839
66. Buck MD, Sowell RT, Kaech SM, Pearce EL. Metabolic Instruction of Immunity. *Cell*. 2017; 169(4):570–86. <https://doi.org/10.1016/j.cell.2017.04.004> PMID: 28475890
67. Pearce EL. Metabolism in T cell activation and differentiation. *Current opinion in immunology*. 2010; 22(3):314–20. <https://doi.org/10.1016/j.coi.2010.01.018> PMID: 20189791
68. Liu G, Xu J, Wu H, Sun D, Zhang X, Zhu X, et al. IL-27 Signaling Is Crucial for Survival of Mice Infected with African Trypanosomes via Preventing Lethal Effects of CD4+ T Cells and IFN-gamma. *PLoS Pathog*. 2015; 11(7):e1005065. <https://doi.org/10.1371/journal.ppat.1005065> PMID: 26222157
69. Klarquist J, Chitrakar A, Pennock ND, Kilgore AM, Blain T, Zheng C, et al. Clonal expansion of vaccine-elicited T cells is independent of aerobic glycolysis. *Science Immunology*. 2018; 3(27):eaas9822. <https://doi.org/10.1126/sciimmunol.aas9822> PMID: 30194241
70. Tarantino G, Scalera A, Finelli C. Liver-spleen axis: intersection between immunity, infections and metabolism. *World journal of gastroenterology*. 2013; 19(23):3534–42. <https://doi.org/10.3748/wjg.v19.i23.3534> PMID: 23801854
71. Yurdakul P, Dalton J, Beattie L, Brown N, Erguven S, Maroof A, et al. Compartment-specific remodeling of splenic micro-architecture during experimental visceral leishmaniasis. *Am J Pathol*. 2011; 179(1):23–9. <https://doi.org/10.1016/j.ajpath.2011.03.009> PMID: 21703391
72. Dalton JE, Glover AC, Hoodless L, Lim EK, Beattie L, Kirby A, et al. The neurotrophic receptor Ntrk2 directs lymphoid tissue neovascularization during *Leishmania donovani* infection. *PLoS Pathog*. 2015; 11(2):e1004681. <https://doi.org/10.1371/journal.ppat.1004681> PMID: 25710496
73. Vander Heiden MG, Cantley LC, Thompson CB. Understanding the Warburg effect: the metabolic requirements of cell proliferation. *Science*. 2009; 324(5930):1029–33. <https://doi.org/10.1126/science.1160809> PMID: 19460998
74. Abboud G, Choi S-C, Kanda N, Zeumer-Spataro L, Roopenian DC, Morel L. Inhibition of Glycolysis Reduces Disease Severity in an Autoimmune Model of Rheumatoid Arthritis. *Frontiers in Immunology*. 2018; 9(1973).
75. Song G, Lu Q, Fan H, Zhang X, Ge L, Tian R, et al. Inhibition of hexokinases holds potential as treatment strategy for rheumatoid arthritis. *Arthritis Res Ther*. 2019; 21(1):87. <https://doi.org/10.1186/s13075-019-1865-3> PMID: 30944034
76. Wilson JJ, Chow KH, Labrie NJ, Branca JA, Sproule TJ, Perkins BRA, et al. Enhancing the efficacy of glycolytic blockade in cancer cells via RAD51 inhibition. *Cancer biology & therapy*. 2019; 20(2):169–82.
77. Choi SC, Titov AA, Abboud G, Seay HR, Brusko TM, Roopenian DC, et al. Inhibition of glucose metabolism selectively targets autoreactive follicular helper T cells. *Nature communications*. 2018; 9(1):4369. <https://doi.org/10.1038/s41467-018-06686-0> PMID: 30348969
78. Yoshida H, Hamano S, Senaldi G, Covey T, Faggioni R, Mu S, et al. WSX-1 is required for the initiation of Th1 responses and resistance to *L. major* infection. *Immunity*. 2001; 15(4):569–78. [https://doi.org/10.1016/s1074-7613\(01\)00206-0](https://doi.org/10.1016/s1074-7613(01)00206-0) PMID: 11672539
79. Mombaerts P, Iacomini J, Johnson RS, Herrup K, Tonegawa S, Papaioannou VE. RAG-1-deficient mice have no mature B and T lymphocytes. *Cell*. 1992; 68(5):869–77. [https://doi.org/10.1016/0092-8674\(92\)90030-g](https://doi.org/10.1016/0092-8674(92)90030-g) PMID: 1547488
80. Kamanaka M, Kim ST, Wan YY, Sutterwala FS, Lara-Tejero M, Galan JE, et al. Expression of interleukin-10 in intestinal lymphocytes detected by an interleukin-10 reporter knockin tiger mouse. *Immunity*. 2006; 25(6):941–52. <https://doi.org/10.1016/j.immuni.2006.09.013> PMID: 17137799

81. Wan YY, Flavell RA. Identifying Foxp3-expressing suppressor T cells with a bicistronic reporter. *Proceedings of the National Academy of Sciences of the United States of America*. 2005; 102(14):5126–31. <https://doi.org/10.1073/pnas.0501701102> PMID: 15795373
82. Stetson DB, Mohrs M, Reinhardt RL, Baron JL, Wang ZE, Gapin L, et al. Constitutive cytokine mRNAs mark natural killer (NK) and NK T cells poised for rapid effector function. *J Exp Med*. 2003; 198(7):1069–76. <https://doi.org/10.1084/jem.20030630> PMID: 14530376
83. Bradley DJ, Kirkley J. Regulation of *Leishmania* populations within the host. I. the variable course of *Leishmania donovani* infections in mice. *Clinical and experimental immunology*. 1977; 30(1):119–29. PMID: 606433
84. Schneider CA, Rasband WS, Eliceiri KW. NIH Image to ImageJ: 25 years of image analysis. *Nature Methods*. 2012; 9:671. <https://doi.org/10.1038/nmeth.2089> PMID: 22930834